

Tetraquarks at large M and large N

Héloïse Allaman ^a, Majid Ekhterachian ^a, Filippo Nardi ^a, Riccardo Rattazzi ^{a,b,c}
and Stefan Stelzl ^a

^aTheoretical Particle Physics Laboratory (LPTP), Institute of Physics, EPFL,
Lausanne, Switzerland

^bCenter for Cosmology and Particle Physics, New York University,
New York, U.S.A.

^cCERN, Theoretical Physics Department,
Geneva, Switzerland

E-mail: heloise@allaman.net, majid.ekhterachian@epfl.ch,
filippo.nardi@epfl.ch, riccardo.rattazzi@epfl.ch, stefan.stelzl@epfl.ch

ABSTRACT: We study tetraquarks in large N QCD with heavy quarks, in the domain where non-relativistic quantum mechanics offers an adequate approximation. Within the regime of validity of the Born-Oppenheimer approximation, we systematically study and explicitly construct tetraquark states. At leading order in the $1/N$ expansion, the bound spectrum consists of free mesons, while the $1/N$ corrections give rise to a Born-Oppenheimer potential that can bind the mesons into tetraquarks. We find two different types of tetraquarks, each endowed with distinct color-spatial wavefunctions. These states arise in the presence of an $\mathcal{O}(N)$ mass hierarchy between the quarks and the antiquarks. We provide a quantitative argument indicating that only for such a hierarchy is the ground state of the system a tetraquark. We discuss what the extrapolation of our results to realistic values of the parameters may imply for the QCD tetraquark states.

KEYWORDS: $1/N$ Expansion, Properties of Hadrons, Quarkonium

ARXIV EPRINT: [2407.18298](https://arxiv.org/abs/2407.18298)

Contents

1	Introduction	1
2	Hamiltonian	5
2.1	The single gluon exchange Hamiltonian	5
2.2	Corrections to the single gluon exchange Hamiltonian	8
3	Tetraquarks within the Born-Oppenheimer approximation: two heavy quarks and two lighter antiquarks	11
3.1	Leading order in $1/N$: the mesons	13
3.2	Subleading in $1/N$: the Born-Oppenheimer potential	14
3.3	Two types of tetraquarks	14
3.4	Tetraquarks with identical quarks: spin-statistics and excited states	19
4	Beyond Born-Oppenheimer	22
4.1	Two heavy quarks and two lighter anti-quarks	22
4.2	Alternative quark mass hierarchies and orderings	27
5	Discussion and speculations about real-world tetraquarks	28
A	Wave functions and the Hamiltonian	31
A.1	The states of a $qq\bar{q}\bar{q}$ system	31
A.2	The potential in different bases	32
B	The Born-Oppenheimer approximation	33
B.1	A large N analog of Hydrogen molecule ion	34
C	Analytic form of the Born-Oppenheimer potential	36
D	Effects of the excited states	36

1 Introduction

Experimental evidence for the existence of exotic hadrons containing four or five valence quarks has been accumulating since the observation of $X(3872)$ [1]. The early candidate four quark states contained a heavy quark anti-quark pair (for reviews, see e.g. [2–5]). More recently, however, states with a $cc\bar{u}\bar{d}$ flavor content, labelled T_{cc}^+ [6, 7], as well as a candidate $cc\bar{c}\bar{c}$ state called $X(6900)$ [8] have also been identified by the LHCb experiment. The nature of all the tetraquark states is still debated. The future experimental program will provide more data on the existing states and may potentially lead to observation of new states such as the analogs of T_{cc} involving one or two b quarks or even states with more than two heavy quarks.

The observed candidate states exhibit the peculiar feature of extreme closeness to the corresponding two meson thresholds. In particular the mass of the $X(3872)$ is within 120 keV

of the $D^0\bar{D}^{*0}$ threshold, and T_{cc}^+ has been observed to have a mass within only around 400 keV of the D^0D^{*+} threshold. Other candidates tetraquarks (e.g. $Z_c(3900)$, $Z_c(4020)$, and $Z_b(10650)$) are also found within ~ 10 MeV of the corresponding two meson threshold. Interpreting these states as compact tetraquarks, one would expect their binding energy to be $O(\Lambda_{\text{QCD}})$, while for loosely bound molecular states one would expect it to roughly scale as Λ_{QCD}^2/M , with M is the mass of the constituent mesons. Nevertheless, in both cases, the extreme closeness to threshold seems to require parametric tuning, tough at different levels.

The ongoing debate on the true nature of tetraquarks, as well as the potential for future experimental progress, strongly motivates studying them within a controlled theoretical framework. It is possible that, in view of the strongly coupled nature of the relevant dynamics, a full clarification will only eventually come with sufficiently accurate lattice QCD simulations. Nonetheless systematic Effective Field Theory (EFT) approaches, like Heavy-Quark Effective Theory (HQET) (see e.g. [9]) or Non Relativistic EFT (see e.g. [10]), will surely always play a central role in the description of both the spectrum and of the phenomenology, illustrations of the former and latter approaches can be found for instance in [11, 12] and [13–15] respectively. Alongside these systematic approaches the large N limit [16] has since long offered a qualitative or semi-quantitative, yet deep, understanding of the strong interactions. The large N limit is normally considered in the strongly coupled regime, involving massless quarks and gluons. In this paper we will instead use it in conjunction with the large quark mass limit. The conjunction of the two limits will allow us to treat analytically, within non-relativistic quantum mechanics, the non-trivial four body bound state problem. That in our mind compensates for the fact that the system we are considering is not fully realistic. Nonetheless lessons for the real world are not excluded.

The existence of narrow tetraquarks in the large N limit of QCD has been under debate during the last decade. Arguments for the absence of such states were originally given by Witten [17] and by Coleman in [18] in their classic papers on the large N expansion. The main argument consists in the observation that in the leading large N approximation the two point function of tetraquark operators factorizes into the disconnected product of meson propagators, so that tetraquark poles are not found in such correlators. That mesons (and baryons) represent the only resonances at infinite N also intuitively matches the fact that mesons are free in that limit, and thus cannot bind into tetraquarks. However in 2013 Weinberg [19] pointed out a potential loophole in the main argument: the connected part of the tetraquark 2-point function, even if subleading in the $1/N$ expansion, may still contain a tetraquark pole. Application of the LSZ approach would then allow to construct the scattering amplitudes involving this state. The main issue in that respect is whether its width is self-consistently suppressed at large N . Indeed an unsuppressed width would offer an additional argument against the existence of tetraquarks. Now, as shown by Weinberg and subsequently analyzed in more detail, the N power counting of the 3-point function for one tetraquark and two mesonic operators shows that the width would, self-consistently, be $1/N$ suppressed. To be more precise, arguments have also been provided indicating that a tetraquark singularity can only exist in diagrams with non-planar topology ([20–22], for reviews see e.g. [23] or [24]). But even in that case the N power counting is consistent with a suppressed width, albeit by a different power of $1/N$. Of course while Weinberg’s remark, and

the works that followed, points to a possible loophole in the arguments against tetraquark, it unfortunately cannot provide a solid argument in favor. Our study is partly motivated by this frustrating state of things. We focus on an admittedly more special situation with the goal to be rewarded with some solid conclusions.

There are different ways to define the large N limit such that the exotic hadrons reduce for $N = 3$ to QCD tetraquarks. In this paper, tetraquarks are bound states involving two quarks in the fundamental representation of $SU(N)$ and two anti-quarks in the anti-fundamental. Another approach is to consider large N QCD with quarks in two-index-antisymmetric representation [25], with tetraquarks made up of two quarks and two antiquarks [26]. Yet another option is to stick to quarks in the fundamental and consider baryonium states, made up of $N - 1$ quarks and $N - 1$ antiquarks as considered already by Witten [17], for a recent discussion see e.g. [27].

We will work in the regime where all quark masses are much above the QCD scale, treating the 't Hooft coupling $\alpha_s N$ as fixed but much smaller than $O(1)$. This will allow us to study tetraquarks benefiting from both the non-relativistic approximation and the $1/N$ expansion. Allowing additionally for a hierarchy among the quark masses will allow us to also employ a controlled Born-Oppenheimer (BO) approximation in the study of bound states. Throughout the paper, we will denote the heavier quarks (antiquarks) with Q (\bar{Q}) and the lighter ones with q (\bar{q}), and we will consider the cases with both different and identical flavors of quarks or antiquarks. We will find that stable $QQ\bar{q}\bar{q}$ tetraquark states with two heavier quarks and two lighter antiquarks can be systematically constructed if the mass hierarchy is larger than $O(N)$. This condition can be understood as follows. At leading order in $1/N$, free mesons are the exact eigenstates of the Hamiltonian while a BO potential for the heavier quarks only arises as a subleading $1/N$ correction. The latter can bind the mesons only if their kinetic energy is similarly suppressed, i.e. if their mass is sufficiently large. In the regime of validity of the BO approximation the ground state of the four quark system is indeed a stable tetraquark. However our construction also entails excited states that are expected to decay mostly into mesons when considering either corrections to the BO approximation or gluon emission. While most of our explicit results pertain the BO regime, in a final section we provide evidence that no exactly stable tetraquark exists outside this regime. We have not systematically studied the possible occurrence of metastable states. But overall our results seem in line with the standard expectation of large N QCD, that mesons (and baryons) are the only bound states, unless some other parameter (in our case the mass hierarchy between quarks and anti quarks) enters the game.

In our analysis we find two types of 4-body bound states with distinct color-coordinate wavefunctions which we refer to as type-I and type-II tetraquarks. In Type-I states the heavy quarks are predominantly in a color anti-symmetric configuration and localized within a region that is much smaller than that where the light anti-quarks are localized. Instead, in type-II states, the average relative distances among the 4 constituents are comparable, and moreover color and position are strongly entangled. Due to the $1/N$ suppression of the BO potentials, the states are parametrically close to the two meson threshold. Moreover for the type-II states we remarkably find a sort of accidental additional closeness to threshold, which originates from the peculiar exponential form of the BO potential.

The type-I tetraquarks are the large N incarnation of states whose existence was established long ago in QCD for heavy enough quarks. In color $SU(3)$ these states can be thought of as baryons made of two (anti-)quarks and a tightly bound heavy diquark. The existence of such states for a large enough mass ratio was first pointed out in the early 80's [28] using a phenomenological potential. The picture of tetraquarks as a compact heavy anti-triplet diquark bound to two light antiquarks, like in a baryon, was painted in [29]. It was then studied systematically in [30] (see also [31]). In the early 2000's, the appearance in the SELEX data [32, 33] of a candidate doubly heavy Ξ_{cc}^+ baryon prompted a first study [34] where a prediction for the T_{cc}^+ mass was made on the basis of a simple quark model using the observed Ξ_{cc}^+ mass. As the SELEX results were later not confirmed by several other experiments, one had to wait for the observation by LHCb in 2017 of the doubly heavy baryon Ξ_{cc}^{++} [35] for the resumption of theoretical activity on this front. That was first undertaken in ref. [36], again on the basis of a simple quark model, for which a systematic study of the uncertainties seems unfortunately not possible. In ref. [11] a more systematic approach based on heavy quark effective theory and quark-diquark symmetry was then undertaken. That was further significantly refined in ref. [12], which includes also a comprehensive evaluation of the errors. Although these works all agree on the existence below the two meson threshold of tetraquarks containing two b quarks (which are the analogue of our type-I states), they don't agree on tetraquarks containing two charm quarks. More precisely ref. [36] predicts the mass of T_{cc} to be within a few MeV from threshold, while refs. [11, 12] predict it $\mathcal{O}(100)$ MeV above, with a comparably small error. But the mass of T_{cc} has in the meantime been measured, and it is perhaps as baffling as anything about tetraquarks that the measured value sits right on threshold, in agreement with the seemingly more qualitative prediction of the quark model, and in disagreement with the prediction of the more systematic heavy quark EFT approach. On the other hand there is still space for further refinement of the HQET analysis, which in its present form neglects effects associated with the finite size of the heavy diquark system. The leading such correction was already estimated in [37] and can significantly affect the mass of T_{cc} . Yet another possibility, suggested by our work, is that the observed T_{cc} is more akin to our loosely bound type II tetraquark than to the deeply bound type I.

The existence of stable tetraquarks at large N with all quark masses large and possibly hierarchical has been previously studied in [38]. There, only the states where the two heavier quarks are bound in a diquark are considered. A hierarchy of masses is also found necessary for the existence of tetraquarks. However the condition they find for the ratio between the quarks and the antiquarks masses is $M/m \gg N^{3/2}$, which is different and stronger than our $M/m \gg N$. We have not been able to sort out the source of disagreement. On the one hand, in their analytic estimate they require specific terms to be small for self-consistency, while we find these terms can be included in a systematic $1/N$ expansion. On the other, their necessary condition for the existence of tetraquarks is ultimately obtained numerically, making it difficult to find the source of disagreement.

In recent years the application of the BO approximation to the study of tetraquarks in real world QCD has started being explored. The grand goal, as outlined for instance in [39] would be to use lattice QCD to compute the BO potential among the heavy constituents. Significant progress has then been made in particular for $QQ\bar{q}\bar{q}$, and apparently less so

in the case of $Q\bar{Q}q\bar{q}$ (see however [40, 41]). In particular [42] computed the potential for two static quarks on the lattice and applied it to the T_{bb} (see ref. [43] for a recent review of the lattice results) finding bound states below threshold. Other studies, perhaps while waiting for more reliable lattice simulations, have relied on phenomenological modelling of the potential (see e.g. [44, 45]). While these approaches are worthy of consideration, our study of the BO approximation in a fully controllable situation indicates the approximations made by these approaches are probably still too crude. For instance ref. [45] works under the assumption of factorized color-coordinate wave functions, while our study shows that the resulting energy eigenstates are often entangled. That is due, as we shall see, to the existence of terms in the Hamiltonian which mix different color singlet configurations and which we can precisely account for.

This paper is organized as follow. In section 2 we write the leading Hamiltonian for the four-quark system and discuss its regime of applicability as well as the main subleading corrections. In section 3 we study the tetraquark states containing two heavy quarks and two lighter antiquarks using the Born-Oppenheimer approximation, showing the existence of two distinct types of tetraquarks. We also study the excited states and the consequences of the spin-statistics theorem for these tetraquarks. In section 4 we extend our study beyond regime of applicability of the BO approximation and argue for non-existence of tetraquark ground states in this regime. In section 5 we discuss to what extent our results may be extrapolated to realistic values of parameters in QCD with $N = 3$ and physical quark masses and what they may imply for the tetraquark states.

2 Hamiltonian

In this section we begin our investigation of the existence of tetraquark states in QCD with a large number of colors N and heavy quark masses by writing the leading Hamiltonian governing the dynamics of the system. We then present a discussion of the subleading corrections which further clarifies the regime of validity of the leading description.

2.1 The single gluon exchange Hamiltonian

A systematic study of the four quark system can be performed in the limit where the quarks are heavy and thus their dynamics is controlled by a non-relativistic Hamiltonian. At large N , the expansion is conveniently organised in terms of $1/N$ and a 't Hooft coupling

$$\alpha = \frac{1}{2}\alpha_s N, \tag{2.1}$$

where $\alpha_s = g_s^2/4\pi$, with g_s being the gauge coupling and the $1/2$ factor is included for later convenience. The strong coupling scale Λ_{QCD} is the scale at which α becomes order unity. We work in the regime where all quark masses are heavy,

$$m_i \gg \Lambda_{\text{QCD}}. \tag{2.2}$$

This implies that $\alpha \ll 1$ evaluated at the relevant scales controlled by m_i . The same parameter α controls gluon emission as well as the relativistic corrections. This can be seen most easily by introducing separate units for space and time and thus reintroducing the speed of light

c. That way the coupling α is conveniently defined as carrying units of velocity. Higher corrections are then controlled by the dimensionless ratio α/c , as systematized within the framework of NRQCD, see e.g. [9]. The truncation to the non-relativistic Hamiltonian, which we shall employ, is then self-consistently justified by taking the formal limit $c \rightarrow \infty$.

The Hamiltonian of the system of two quarks and two anti-quarks, labeled respectively with indices $1 - 2$ and $\bar{3} - \bar{4}$, is then given by

$$H = \sum_i \frac{p_i^2}{2m_i} + \sum_{i < j} \alpha_s \frac{T_{(i)}^a T_{(j)}^a}{r_{ij}} + \text{small corrections}, \quad \text{for } r_{ij} \ll \Lambda_{\text{QCD}}^{-1}, \quad (2.3)$$

where $r_{ij} = |\vec{r}_i - \vec{r}_j|$ are the relative distances between particles i and j . We consider the quarks to be in the fundamental representation of the $SU(N)$ gauge group. The T^a matrices are the $N^2 - 1$ generators of the $SU(N)$ color group in the (anti-) fundamental representation for (anti-) quarks. The pairwise Coulomb interactions are at most of order α/r_{ij} (see appendix A for more details). Let us note that, because at short distances the running of the 't Hooft coupling is very slow, it is self-consistent to neglect its scale dependence and choose its scale a posteriori as the typical size of the bound state. Some care has to be taken if the state is characterized by parametrically separated scales.

The state of two heavy quarks and two heavy anti-quarks can be defined by assigning their position and their color state, as well as their flavor and spin. The possible color states come from the tensor product of two fundamental and two anti-fundamental representations of $SU(N)$. This gives rise to two singlets, two adjoints, and four other colored representations given by the tensor product of two adjoints. We restrict our analysis to the color singlet subspace, as we expect the ground state to lie in this sector. In the next section we will show that is indeed the case, at least for a specific hierarchy of quark masses. We then write a generic state of the system in the form

$$|\Psi\rangle = \sum_{\rho} \int \prod_{k=1}^4 d^3 r_k \Psi_{m n}^{i j}(r, \rho) |1_i(r_1, \rho_1) 2_j(r_2, \rho_2) \bar{3}^m(r_{\bar{3}}, \rho_{\bar{3}}) \bar{4}^n(r_{\bar{4}}, \rho_{\bar{4}})\rangle, \quad (2.4)$$

with $\Psi_{m n}^{i j}$ invariant under the action of $SU(N)$ on the color indices (i, j, m, n) . We have also collectively denoted the flavor and spin quantum numbers by ρ . The wave function must be localized inside the region $r_{ij} \ll \Lambda_{\text{QCD}}^{-1}$ for its dynamics to be controlled by the Hamiltonian in (2.3). As there exist two independent color singlet contractions of the four color indices, the wave function spans a two-dimensional subspace. Different choices for the basis of this subspace can be made, with their convenience depending on the question being asked and the regime being considered. (for a more detailed exposition see appendix A). One possibility is to pick a basis where one element corresponds to a pair of $q\bar{q}$ singlets, while the orthogonal element corresponds to a state where the same $q\bar{q}$ pairs lie in the adjoint representation. Obviously, there exist two such options, corresponding to the two possible pairings, either $1\bar{3}$ and $2\bar{4}$ or $1\bar{4}$ and $2\bar{3}$. A more “symmetric” basis is obtained by first considering the two states where the qq lie in either a color symmetric (Ψ_S) or anti-symmetric (Ψ_A) configuration, with the $\bar{q}\bar{q}$ pair in the conjugate representation so as to make up a singlet, and by then forming the combinations

$$\Psi_+ = \frac{1}{\sqrt{2}}(\Psi_S + \Psi_A), \quad \Psi_- = \frac{1}{\sqrt{2}}(\Psi_S - \Psi_A). \quad (2.5)$$

In color space the potential is then given by a two dimensional matrix,

$$V = \begin{pmatrix} V_{++} & V_{-+} \\ V_{+-} & V_{--} \end{pmatrix} \tag{2.6}$$

with elements (see appendix A.2)

$$\begin{aligned} V_{++} &= -\frac{\alpha}{r_{1\bar{3}}} - \frac{\alpha}{r_{2\bar{4}}} + \mathcal{O}\left(\frac{1}{N^2}\right), \\ V_{+-} = V_{-+} &= \frac{\alpha}{2N} \left(\frac{2}{r_{12}} + \frac{2}{r_{3\bar{4}}} - \frac{1}{r_{1\bar{3}}} - \frac{1}{r_{1\bar{4}}} - \frac{1}{r_{2\bar{3}}} - \frac{1}{r_{2\bar{4}}} \right) + \mathcal{O}\left(\frac{1}{N^2}\right), \\ V_{--} &= -\frac{\alpha}{r_{1\bar{4}}} - \frac{\alpha}{r_{2\bar{3}}} + \mathcal{O}\left(\frac{1}{N^2}\right). \end{aligned} \tag{2.7}$$

The $N \rightarrow \infty$ limit, with the quark masses kept fixed, is manifest. The mixing between the singlets vanishes and the diagonal elements consists of just two $q\bar{q}$ Coulombic potentials. In this limit,

$$\begin{aligned} \Psi_+ &\rightarrow (1\bar{3})_{\text{singlet}}(2\bar{4})_{\text{singlet}}, \\ \Psi_- &\rightarrow (1\bar{4})_{\text{singlet}}(2\bar{3})_{\text{singlet}}, \end{aligned} \tag{2.8}$$

and the spectrum corresponds to that of two free mesons for both possible pairings. When N is large but finite, the physics of this system is richer. In particular, we will show that the $1/N$ corrections can form tetraquark states in specific regimes of the particles masses. Since in the Hamiltonian in eq. (2.3), we keep the $1/N$ corrections and neglect the α^2 ones, it naively seems to be necessary to impose $\alpha \ll 1/N$. However, as we will show below, this is not the case. The leading interactions in $1/N$, to any order in α , only modify the Coulombic interactions among the pairs of quark anti-quark binding into mesons when $N \rightarrow \infty$. Thus they do not give rise to interactions among the two pairs. Indeed, they correspond to diagrams with the two-meson topology that is two fermion loops that must be disconnected in order to survive in the $N \rightarrow \infty$ limit. A more detailed large N counting is provided in the next section. For our purposes, the knowledge of the $q\bar{q}$ interactions at leading order in α will be sufficient to compute the distance from threshold of the tetraquark states to first order in α and in $1/N$.

We will then be interested in the study of the bound states of this system as a function of the particle masses in the region where we can gain some analytic understanding. To this purpose, the Hamiltonian previously defined is too complicated as it generically entails the solution of a four-body problem. The dynamics can be simplified if we consider the regime with a mass hierarchy between the four particles. More specifically, we will study the situation where two of them are heavier, with masses of order M while the other two have a mass of order m with $\Lambda_{\text{QCD}} \ll m \ll M$. Up to charge conjugation, there are two classes of systems, that where two quarks are heavy, denoted as $QQ\bar{q}\bar{q}$, with masses $M_1, M_2 = \mathcal{O}(M)$ and $m_{\bar{3}}, m_{\bar{4}} = \mathcal{O}(m)$, and that where the heavy particles are a quark and an anti-quark $Q\bar{Q}q\bar{q}$ with $M_1, M_{\bar{3}} = \mathcal{O}(M)$ and $m_2, m_{\bar{4}} = \mathcal{O}(m)$. The hierarchy $m/M \ll 1$ does not guarantee by itself the separation between two dynamical scales as these are determined by the structure of the interactions and the reduced masses of the system. Indeed only for the $QQ\bar{q}\bar{q}$ case do we find self-consistent bound states in an expansion in powers of m/M . At leading order,

one can first solve for the dynamics of the light particles with the heavy ones providing a static background and then use the solution to generate an effective potential for the heavy quarks. This is the Born-Oppenheimer approximation which will be shown to be valid as long as $m/M < 1/N$.

As the mass hierarchy becomes larger $m/M \lesssim 1/N^2$, the heavy quarks eventually dominate the binding energy of the lowest-lying states and their dynamic becomes faster than that of the anti-quarks. For this reason, it is convenient to use a basis of states with a definite color configuration of the quarks. These can either be in a symmetric or an anti-symmetric configuration. The matrix elements of the potential in this basis are

$$\begin{aligned}
 V_{SS} &= -\frac{\alpha}{2} \left(\frac{1}{r_{1\bar{3}}} + \frac{1}{r_{1\bar{4}}} + \frac{1}{r_{2\bar{3}}} + \frac{1}{r_{2\bar{4}}} \right) \\
 &\quad + \frac{\alpha}{2N} \left(\frac{2}{r_{12}} + \frac{2}{r_{\bar{3}\bar{4}}} - \frac{1}{r_{1\bar{3}}} - \frac{1}{r_{1\bar{4}}} - \frac{1}{r_{2\bar{3}}} - \frac{1}{r_{2\bar{4}}} \right) + \mathcal{O}\left(\frac{1}{N^2}\right), \\
 V_{SA} = V_{AS} &= -\frac{\alpha}{2} \left(\frac{1}{r_{1\bar{3}}} + \frac{1}{r_{2\bar{4}}} - \frac{1}{r_{1\bar{4}}} - \frac{1}{r_{2\bar{3}}} \right) + \mathcal{O}\left(\frac{1}{N^2}\right), \\
 V_{AA} &= -\frac{\alpha}{2} \left(\frac{1}{r_{1\bar{3}}} + \frac{1}{r_{1\bar{4}}} + \frac{1}{r_{2\bar{3}}} + \frac{1}{r_{2\bar{4}}} \right) \\
 &\quad - \frac{\alpha}{2N} \left(\frac{2}{r_{12}} + \frac{2}{r_{\bar{3}\bar{4}}} - \frac{1}{r_{1\bar{3}}} - \frac{1}{r_{1\bar{4}}} - \frac{1}{r_{2\bar{3}}} - \frac{1}{r_{2\bar{4}}} \right) + \mathcal{O}\left(\frac{1}{N^2}\right).
 \end{aligned}
 \tag{2.9}$$

In this regime, one can thus solve first for the states of the heavy pair, which bind at short distances in an anti-symmetric state, and then consider the system of the compact diquark interacting with the two anti-quarks.

2.2 Corrections to the single gluon exchange Hamiltonian

In this subsection we discuss why we can include the interactions of order α/N in eq. (2.3) while dropping terms of $\mathcal{O}(\alpha^2)$ without assuming a hierarchy between the 't Hooft coupling α and $1/N$. We also justify why we can limit our analysis to the singlet subspace. The reader who is satisfied with these statements can directly skip to section 3.

To power count the different contributions to the Hamiltonian of the system, we study the position space propagator of the two quarks and two anti-quarks. This is expanded in diagrams with four incoming and four outgoing fermion lines each of which carries either a fundamental or an anti-fundamental color index. These indices will be contracted with the ones of the wave functions of the possible color states of the quarks and anti-quarks. To proceed in the usual counting of powers of N , we thus need to give a diagrammatic representation for the external states. This is easily done once the color wave functions are known. Indeed, they are constructed in terms of Kronecker deltas δ_j^i , and the generators of the fundamental representation $(T^a)_j^i$ for which the double line notation is the canonical one used in large N . As an example, consider the color state of a $q\bar{q}$ pair, this can be either a singlet or one of the $N^2 - 1$ states of the adjoint representation. The wave functions are given by $\frac{1}{\sqrt{N}}\delta_j^i$ and $\sqrt{2}(T^a)_j^i$ respectively. The diagrammatic contraction with a quark and an anti-quark line is represented in figure 1.

As for the system of two quarks and two anti-quarks, the tensor product of two fundamental and two anti-fundamental representations in $SU(N)$ gives rise to two singlets, two adjoints,

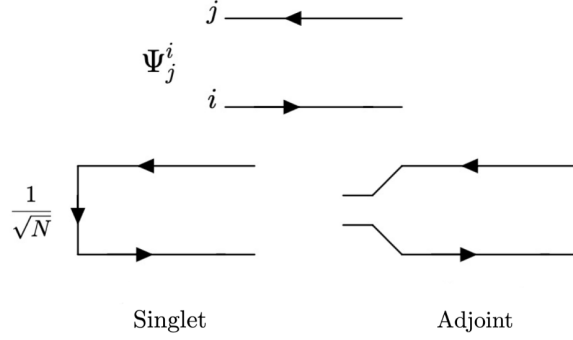


Figure 1. Diagrammatic representation of the color wave functions of a $q\bar{q}$ system. The open color line represents an adjoint index labeling the possible $N^2 - 1$ states in the representation.

and four other colored representations coming from the tensor product of two adjoints. We start studying the order of the corrections within the singlet subspace, before studying the mixing with higher dimensional representations in the next subsection. For the ease of the reader, let us recall some of the results in the large N counting that will use in the following.

- The leading contribution in $1/N$ is a sum of diagrams whose boundary is defined by fermion lines and planar gluons decorate its interior.
- Non planar gluon corrections come in powers of $1/N^2$.
- Internal quark loops are suppressed by $1/N$ with respect to a gluon loop with the same topology. For this reason, they can be neglected.

2.2.1 Singlet subspace

Let us start studying the Hamiltonian in the singlet subspace. The wave-functions for the states defined in (2.5) to sub-leading order in $1/N$ are (see appendix A)

$$\begin{aligned}
 P(+)^{ij}_{mn} &\equiv P(S)^{ij}_{mn} + P(A)^{ij}_{mn} = \frac{\sqrt{2}}{N} \delta_m^i \delta_n^j + \frac{1}{\sqrt{2}N^2} \delta_n^i \delta_m^j + \mathcal{O}\left(\frac{1}{N^3}\right), \\
 P(-)^{ij}_{mn} &\equiv P(S)^{ij}_{mn} - P(A)^{ij}_{mn} = \frac{\sqrt{2}}{N} \delta_n^i \delta_m^j + \frac{1}{\sqrt{2}N^2} \delta_m^i \delta_n^j + \mathcal{O}\left(\frac{1}{N^3}\right).
 \end{aligned}
 \tag{2.10}$$

As shown in figure 2, we see that the diagrams contributing to the diagonal elements of the Hamiltonian, at leading order in $1/N$, are made of two fermion loops. Other structures of fermion lines are suppressed at least by $1/N^2$. This effect comes either from the wave function factor (as in the rightmost diagram of figure 2) or from the combined contribution of the topology of the diagram and the wave function (as in the middle diagrams of the figure). The two fermion loops must then be decorated with gluons in all possible ways. There are two types of decorations. The ones connecting the loops and the ones that don't. One diagram of each type is shown in figure 4. The former, besides additional powers of the 't Hooft coupling, are $1/N^2$ suppressed. The latter, on the contrary, give rise to α corrections to the SGE Hamiltonian at leading order in $1/N$. However, they all share the structure of a two meson state and they will not generate interactions between the mesons that can compete with

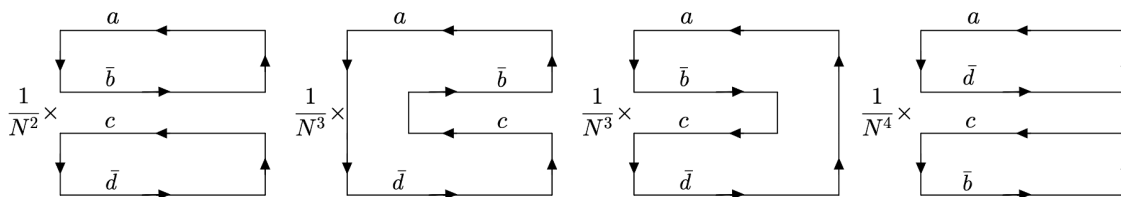


Figure 2. Structure of the fermion lines of the diagrams contributing to the diagonal entries of the Hamiltonian in the basis (2.5). The explicit factors of $1/N$ come from the wave functions (2.10). The letters denote which fermion is related to that line of the propagator. For the $++$ component we have $a = 1, \bar{b} = 3, c = 2, \bar{d} = 4$ while $a = 1, \bar{b} = 4, c = 2, \bar{d} = 3$ for the $--$ one. When decorated with gluons, each diagram gives at most a contribution of the order of the wave-function prefactor multiplied by N to the power of the number of fermion loops.

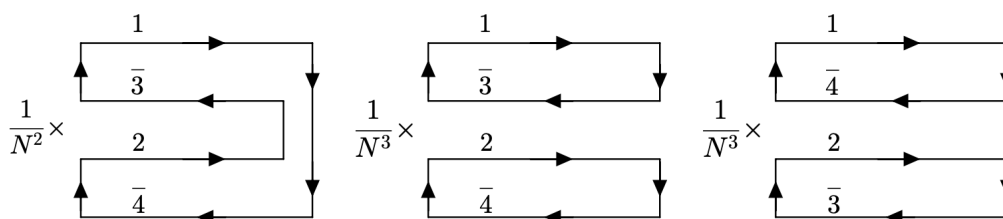


Figure 3. Structure of the leading diagrams contributing to the off-diagonal entries of the Hamiltonian in the basis (2.5). The wave function factor ($1/N^2$ for the first diagram and $1/N^3$ for the other two diagrams) combines with the factors coming from the fermion loops (N for the first diagram, N^2 for the other two) to give the term in equation (2.7).

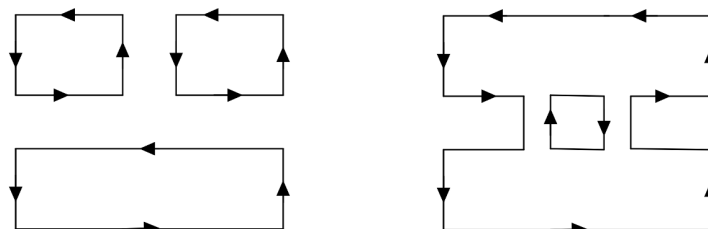


Figure 4. Examples of planar (left) and non planar (right) gluon corrections to the first diagram in figure 2. The diagram on the left contribute at order α while the one on the right gives a contribution of order α^2/N^2 .

the off-diagonal ones at order α/N . We then conclude that the corrections to the diagonal elements of the single gluon exchange Hamiltonian that give rise to interactions among the mesons come at order $1/N^2$. As regards the off-diagonal element, the one in (2.7) is the leading one. Indeed, the dominant diagrams in $1/N$ are shown in figure 3.

2.2.2 Mixing with higher dimensional representations

As we stated before, we expect the ground state of the system to be dominantly in the singlet subspace. In some special cases, this is easy to see. For example in the mass

hierarchy $M_{1,2} \gg N^2 m_{\bar{3}} \gg N^2 m_{\bar{4}}$, the problem reduces to a series of two-body problems that we can easily analyze. The leading order problem consists of two heavy quarks, and the binding energy is maximal if the two heavy quarks forming a compact color anti-symmetric diquark. Then including the lighter anti-quarks one-by-one we can see that the configuration maximizing the binding energy is a total color-singlet. A similar conclusion is found for $N^2 m_{\bar{4}} \gg M_{1,2} \gg N m_{\bar{3}} \gg N m_{\bar{4}}$. This time the binding energy of the full system is dominated by forming the color singlet meson involving \bar{q}_3 , while the leading corrections come from forming the meson involving \bar{q}_4 . The full system is therefore in the color singlet subspace, up to small corrections. From now on we assume that the ground state is dominantly a color singlet, and investigate the mixing with the other color representations.

Besides the singlets, the two quarks and two anti-quarks can lie in higher dimensional representations where the color is neutralized by additional gluons. The tensor product $N \otimes N \otimes \bar{N} \otimes \bar{N}$ gives rise to two adjoint representations and four other irreducible representations whose color must be screened by at least two gluons. If the color is neutralized at the length scale $\Lambda_{\text{QCD}}^{-1}$, we expect any mixing to be suppressed by powers of $\Lambda_{\text{QCD}}/\alpha m$ with m denoting collectively the mass of the quarks. However, if the gluons can localize at a much shorter scale, binding the quarks with the anti-quarks, we expect the mixing to be suppressed only by powers of the weak coupling $\alpha(\text{binding scale})^{1/2}$. At least one power is needed for the adjoint states while two are needed for the others. Nevertheless corrections that survive as $N \rightarrow \infty$, can only give rise to interactions that modify the Coulombic potential between a quark/anti-quark pair. This stems from the fact that the topology of the diagrams associated with interactions among the “mesons” necessarily corresponds to sub-leading order in $1/N$, just as above for the corrections within the singlet sector. Said differently, they only modify the meson states of the $N \rightarrow \infty$ Hamiltonian mixing the $q\bar{q}$ singlet with $q\bar{q} + \text{gluons}$ at some sub-leading order in α . Therefore, for the purpose of determining the leading interaction among the “mesons”, it is sufficient to consider the singlet subspace.

3 Tetraquarks within the Born-Oppenheimer approximation: two heavy quarks and two lighter antiquarks

In this section, we begin our analysis of the Hamiltonian of eq. (2.3) focusing on a specific mass hierarchy, where the quarks are much heavier than the antiquarks. We first focus on the case where all quark flavors are different, while the case where quarks or antiquarks are of the same flavor will be discussed in section 3.4.

Denoting the masses of the quarks by M_1 and M_2 and those of the antiquarks by $m_{\bar{3}}$ and $m_{\bar{4}}$, our starting assumption is then¹

$$M_1 \geq M_2 \gg m_{\bar{3}} \geq m_{\bar{4}} \gg \Lambda_{\text{QCD}}. \tag{3.1}$$

As it will become clear below, it is convenient to introduce the following coordinates

$$\vec{R}_{CM} = \frac{M_1 \vec{r}_1 + M_2 \vec{r}_2 + m_{\bar{3}} \vec{r}_3 + m_{\bar{4}} \vec{r}_4}{M_1 + M_2 + m_{\bar{3}} + m_{\bar{4}}}, \tag{3.2}$$

$$\vec{R} = \vec{r}_2 - \vec{r}_1, \tag{3.3}$$

¹The case where the antiquarks are much heavier than the quarks is simply related to this one by charge conjugation.

$$\vec{r}'_3 = \vec{r}_3 - \frac{\vec{r}_1 + \vec{r}_2}{2}, \tag{3.4}$$

$$\vec{r}'_4 = \vec{r}_4 - \frac{\vec{r}_1 + \vec{r}_2}{2}, \tag{3.5}$$

with their corresponding momenta denoted by \vec{P}_{CM} , \vec{P} , \vec{p}'_3 , and \vec{p}'_4 . Galilean invariance ensures the decoupling of the dynamics of the center of mass (CM) canonical pair $(\vec{R}_{CM}, \vec{P}_{CM})$. For the bound state problem we then need to consider only \vec{R} , \vec{r}'_3 , \vec{r}'_4 and their conjugated momenta. Notice that $\vec{r}'_{3/4}$ are simply the distances of the light anti-quarks from the midpoint of quark 1 and 2, which can be interpreted as a sort of center of color charge. This choice has been made for later convenience. In these coordinates, the Hamiltonian reads

$$H = \frac{P_{CM}^2}{2(M_1 + M_2 + m_3 + m_4)} + \frac{P^2}{2M_{12}} + \frac{p_3'^2}{2m_3} + \frac{p_4'^2}{2m_4} + V + \text{corrections}, \tag{3.6}$$

with $M_{12} \equiv M_1 M_2 / (M_1 + M_2)$ the reduced mass of the heavy quark system. The corrections not written explicitly above consist of terms of the form $\frac{P p_i'}{M}$ and $\frac{p_j' p_i'}{M}$, where M is a heavy quark mass. We will see below that within the Born-Oppenheimer approximation these terms can be consistently dropped.

To apply the Born-Oppenheimer approximation (see e.g. [46] and appendix B), we first focus on a reduced Hamiltonian for the light antiquarks

$$H_R = \frac{p_3'^2}{2m_3} + \frac{p_4'^2}{2m_4} + V, \tag{3.7}$$

where we neglect all the (kinetic) terms suppressed by the heavy quark masses, and where we treat \vec{R} , which appears in V , as a classical parameter.

The energy eigenvalues and eigenstates of the reduced Hamiltonian, satisfying

$$H_R |\psi_{\mathcal{A}}\rangle = E_{\mathcal{A}} |\psi_{\mathcal{A}}\rangle, \tag{3.8}$$

with \mathcal{A} a collective quantum number, can then be found working in a $1/N$ expansion. The eigenvalues $E_{\mathcal{A}}$, with their dependence on \vec{R} , then provide the BO potential for the Q_1 - Q_2 system. More precisely, each light quark state $|\psi_{\mathcal{A}}\rangle$, leads to an approximate effective Hamiltonian

$$H_{BO} = \frac{P^2}{2M_{12}} + E_{\mathcal{A}}(R) \tag{3.9}$$

whose Schrödinger equation provides the approximate wavefunctions and energy levels of the bound 4-quark system. Notice that H_R is invariant under rotations when treating the parameter \vec{R} as a vector. Therefore its eigenvalues can only be functions of the norm $|\vec{R}| \equiv R$, corresponding to a spherically symmetric BO potential.

A crucial final step is to check for the self-consistency of the BO approximation. A simple example of the BO approximation for a molecule with large charge nuclei, where a systematic analysis can be performed analytically, is presented in appendix B.1. The approximation is valid if the motion of the heavy quarks has negligible influence on the wavefunction of the light antiquarks. As also reviewed in appendix B.1, that happens to be the case when

the heavier quarks are much more localized than the lighter antiquarks, or, equivalently, in terms of their momenta (see eq. (3.6))

$$P \gg p'_{3,4}. \tag{3.10}$$

That is also the same condition that allows us to drop the corrections to the kinetic terms in eq. (3.6). As we will show, it reduces in our case to a condition on the masses:

$$M_2 \gg Nm_3. \tag{3.11}$$

The scaling with N comes from the fact that the BO potential is only generated at subleading order in $1/N$, while at leading order, the energy eigenstates are a set of approximately color-singlet free “mesons”.

In the regime of eq. (3.11), we find two distinct tetraquark solutions, while in the regime $m_3 \ll M_2 \ll Nm_3$ we show that there are no tetraquark bound states within the domain of validity of the BO approximation. In section 4, we offer a general argument indicating that in this other regime the ground state is a two meson state and not a tetraquark.

3.1 Leading order in $1/N$: the mesons

In this subsection, we study the reduced H_R Hamiltonian of eq. (3.7), at leading order in $1/N$. In the $+/-$ basis of eq. (2.7) the potential matrix then becomes

$$V = \alpha \begin{pmatrix} -\frac{1}{r_{1\bar{3}}} - \frac{1}{r_{2\bar{4}}} & 0 \\ 0 & -\frac{1}{r_{1\bar{4}}} - \frac{1}{r_{2\bar{3}}} \end{pmatrix} + \mathcal{O}(\alpha/N). \tag{3.12}$$

The Hamiltonian with the leading order potential is straightforward to solve and simply gives rise to two pairs of free “mesons”: $(Q_1\bar{q}_3)$ and $(Q_2\bar{q}_4)$ with the $+$ color configuration and $(Q_2\bar{q}_3)$ and $(Q_1\bar{q}_4)$ in the $-$ configuration. Indeed the $+$ ($-$) states, up to $1/N$ corrections, correspond to configurations where Q_1 and Q_2 form singlets with \bar{q}_3 (\bar{q}_4) and \bar{q}_4 (\bar{q}_3) respectively. H_R has then two degenerate ground states, corresponding to the two different meson pairs. Their energy E_0 is simply given by

$$E_0 = -\mathcal{E}_3 - \mathcal{E}_4 \quad \text{with} \quad \mathcal{E}_3 = \frac{1}{2}\alpha^2 m_3 \quad \text{and} \quad \mathcal{E}_4 = \frac{1}{2}\alpha^2 m_4, \tag{3.13}$$

with \mathcal{E}_3 and \mathcal{E}_4 respectively the binding energies of the meson involving \bar{q}_3 and \bar{q}_4 . The mesons have Bohr radii

$$a_3 = (\alpha m_3)^{-1}, \quad \text{and} \quad a_4 = (\alpha m_4)^{-1}. \tag{3.14}$$

Note that in the BO approximation, the heavy quarks Q_1 and Q_2 are treated as static, and thus in the above equations it is indeed m_3 and m_4 that appears and not the respective reduced masses. It is clear that within the BO approximation, at this order in $1/N$, the energy eigenvalues are independent of the position of the heavy quarks and no BO potential is generated. Moreover, at this order there is a degeneracy between the energy eigenvalues in $+$ and $-$ color configurations. As we shall now see, this degeneracy is broken by the $1/N$ corrections which also gives rise to a BO-potential that can bound the heavy mesons together.

3.2 Subleading in $1/N$: the Born-Oppenheimer potential

According to the discussion in the previous subsection, at leading order in $1/N$ the ground state of the lighter quark dynamics is independent of $R \equiv r_{12}$ and has a two-fold degeneracy. We denote the two ground states by $|\psi_0^\pm\rangle$, with \pm superscript specifying their color configuration. The subleading $1/N$ effects split the degeneracy by an R -dependent correction, with the resulting ground state being a linear combination of the two initially degenerate states. In order to study that, we first compute the matrix element of the potential between the two (degenerate) leading order ground states,

$$\frac{\Delta(R)}{N} = \langle \psi_0^+ | V_{+-} | \psi_0^- \rangle, \quad (3.15)$$

where we factored out a $1/N$ so that $\Delta(R)$ does not scale with N . In terms of this matrix element and of the leading order ground state energy, $E_0 = -\mathcal{E}_3 - \mathcal{E}_4$, the energy eigenvalues are $E_0 \pm \frac{\Delta(R)}{N}$ and correspond to the states $|\psi_0^+\rangle \pm |\psi_0^-\rangle$. The BO potentials (with the free meson energies subtracted) for $|\psi_0^+\rangle \pm |\psi_0^-\rangle$ are therefore simply given by $V_{\text{eff,BO}}^\pm(R) = \pm \frac{\Delta(R)}{N}$. In figure 5, we show $\Delta(R)$ for various choices of $\frac{m_4}{m_3}$. In the limit $\frac{m_4}{m_3} \rightarrow 0$, it takes the following simple analytic form

$$\frac{\Delta(R)}{\mathcal{E}_3} \Big|_{m_4/m_3 \rightarrow 0} = 2e^{-R/a_3} \left(\frac{a_3}{R} - \frac{2}{3} \frac{R}{a_3} \right). \quad (3.16)$$

For $R \ll a_3$ this is well approximated by a repulsive $\propto \frac{1}{R}$ potential, clearly resulting from the $\frac{1}{r_{12}}$ interaction between Q_1 and Q_2 . At $R \gg a_3$, the overlap of the spatial wavefunction of the states is exponentially suppressed and so is $\Delta(R)$. These asymptotic behaviors also hold for generic $\frac{m_4}{m_3}$. The dependence of the curves on $\frac{m_4}{m_3}$ can also be understood as follows. As we increase $\frac{m_4}{m_3}$, the overlap $|\Delta(R)|$ drops faster at large R because of the more spatially localized \bar{q}_4 wavefunction. On the other hand, at small $R \lesssim a_3$, the same increased localization of \bar{q}_4 boosts the negative contribution to $\Delta(R)$ of the terms proportional to $\frac{1}{r_{14}}$ and $\frac{1}{r_{24}}$ in V_{+-} (see eq. (2.7)), thus leading to a smaller $\Delta(R)$. The analytic expression for $\Delta(R)$ expanded up to second order for $m_4/m_3 \ll 1$ is given in the appendix C. For $m_4/m_3 \ll 1$, $\Delta(R)$ is dominated by the contribution from m_3 , so that the results become independent of m_4 . In particular they are unaffected by m_4 being bigger or smaller than Λ_{QCD} .

We can easily see from figure 5, that the BO potential can potentially give rise to two distinct tetraquark bound states: one on the $(-)$ branch where $V_{\text{eff,BO}}^- = -\frac{\Delta(R)}{N}$ provides at $R \ll a_3$ an attractive $\propto \frac{1}{R}$ potential that can localize the two heavy quarks, and the other on the $(+)$ branch where $V_{\text{eff,BO}}^+ = +\frac{\Delta(R)}{N}$ has a minimum around $R \sim a_3$. We discuss these possibilities in detail in the next subsection. So far, the discussion only involved the two ground states of the LO Hamiltonian, however, similar BO potentials arise for excited states, some of which will be discussed in section 3.4.

3.3 Two types of tetraquarks

Having found the BO potentials, we now discuss the possibility of having 4-quark bound states. We will first show that for $M_2 \gg Nm_3$ two distinct sets of tetraquarks exist, with states below the two-meson thresholds in both sets. We will then argue that there are no tetraquark bound states, identifiable under the lamppost of the BO approximation, for $M_2 \ll Nm_3$.

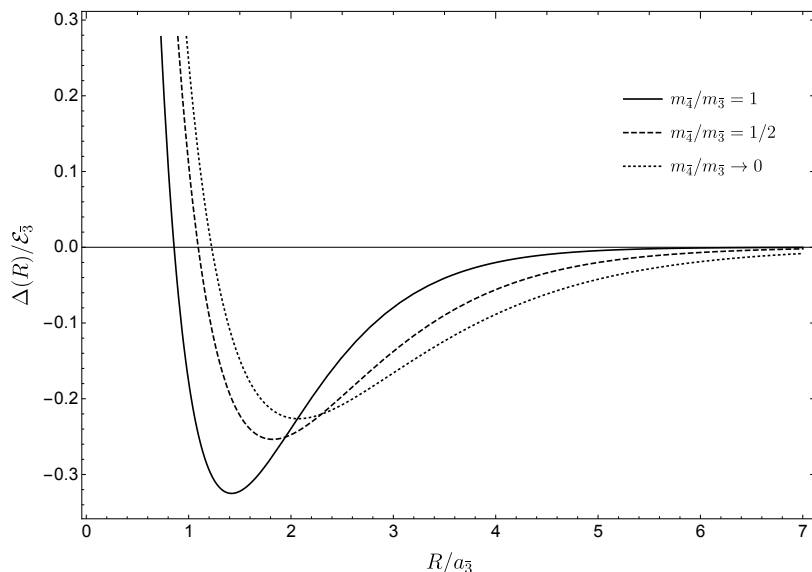


Figure 5. $\Delta(R)/\mathcal{E}_3$ for different values of m_4/m_3 . One can see the minimum at $R \sim O(a_3)$, which leads to type-II tetraquarks, as well as the $1/R$ behaviour at small distances that gives rise to type-I tetraquarks.

With the BO potential found in the previous subsection and including the kinetic terms of the heavy quarks, we can now solve for the dependence of the wavefunction of the energy eigenstates on the heavy quark coordinates. This is a two-body problem with a potential dependent only on the relative distance, which can be reduced to a one-body problem with a central potential for the relative coordinate R .

Type-I tetraquarks. We first consider the $(-)$ branch where the potential $V_{\text{eff,BO}}^- = -\frac{\Delta(R)}{N}$ is attractive at $R \lesssim a_3$. That can give rise to bound states where the heavy quarks are localised much closer to each other than to the lighter antiquarks. We call such states type-I tetraquarks. At $R \ll a_3$, the BO potential is $\sim -\frac{1}{N} \frac{\alpha}{R}$ so that the possible energy eigenstates would be localised within a radius

$$A_{12} \equiv N(\alpha M_2)^{-1} = a_3 \frac{N m_3}{M_2}. \quad (3.17)$$

The BO condition in eq. (3.10) reads $A_{12} \ll a_3$, which by the above equation implies $\frac{M_2}{m_3} \gg N$. The same condition also ensures that the resulting $\sim \frac{\alpha^2}{N^2} M_2$ binding energy is much larger than \mathcal{E}_3/N . Consequently the energy of these states

$$E_{\text{type-I}} = E_0 - \mathcal{O}\left(\frac{\alpha^2}{N^2} M_2\right) \quad (3.18)$$

not only falls well below the two meson threshold, but also below the minimum of the BO potential in the $(+)$ branch and hence below the energy of any bound state that may exist in that other branch. Therefore for $M_2 \gg N m_3$, the ground state of the 4-quark system under study is a tetraquark with the heavier quarks bound together at distances much shorter than the size of the mesons involving the lighter quarks. Notice that $|\psi_0^+\rangle$ and $|\psi_0^-\rangle$ have different

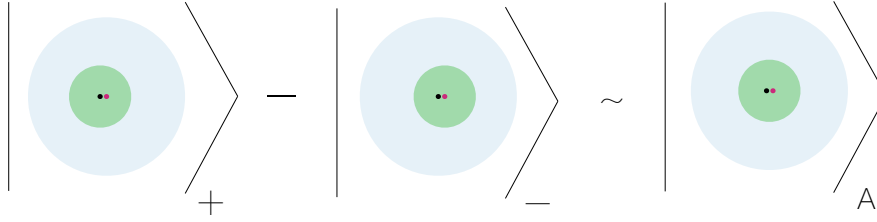


Figure 6. Sketch of type I tetraquark. The black and red dots represent the heavier quarks and the colored regions are where the wavefunction of the lighter antiquarks have a significant support. The “+” and “-” subscripts denote the color configuration of the state, as defined in eq. (2.5). We also indicate the large overlap with the state with the two heavy quarks in the antisymmetric color representation.

color structure and generically different coordinate dependence, so that generically $|\psi_0^+\rangle - |\psi_0^-\rangle$ is an entangled superposition of color and spacial variables. However, the type-I bound states are non-generic superpositions where the two heavy quarks are localized in a small region of size $A_{12} \ll a_{\bar{3}}$. That leads to factorization of color and position up to $O(A_{12}/a_{\bar{3}})$ corrections, with the two heavy (and two light) quarks lying in the anti-symmetric color state (see eq. (2.5)). A schematic sketch of the type-I tetraquark wavefunctions is shown in figure 6.

In the regime of still heavier quarks $M_2 \gg N^2 m_{\bar{3}}$, one can establish the existence of type-I states even without using the BO approximation, see e.g. [11, 31]. In this regime, one can first solve the dynamics of system of two heavier quarks, where one finds deeply bound diquark states in the antisymmetric representation. As the quark-quark potential is roughly $-\frac{\alpha}{Nr_{12}}$, the resulting binding energy $E_{12} \sim \alpha^2 \frac{M_2}{N^2}$ dominates over all other possible contributions to the energy of the four quark system, as they are all $\lesssim \mathcal{E}_{\bar{3}} \sim \alpha^2 m_{\bar{3}}$. Moreover, and relatedly, the time scale associated to motion in the diquark system, $\sim \left(\alpha^2 \frac{M_2}{N^2}\right)^{-1}$, is much shorter than the time scale associated to the motion of the lighter anti-quarks. One can therefore integrate out the diquark dynamics first and then solve the effective dynamics of the system composed of the diquark and the two antiquarks. Nevertheless we can find this state consistently also within the BO approximation, as the dynamics of the heavy quarks has negligible influence on the light antiquarks, since they are localized in a small region. This is against the common lore according to which the BO approximation corresponds to integrating out the faster dynamics of the light particles. The unique color-singlet configuration out of the antisymmetric diquark and the two antifundamental antiquarks has a binding potential and leads to a bound state of the three constituents.² One can solve easily for the wavefunction of such states; at leading order in $1/N$, the antiquarks only interact with the diquark and not with each other (see equation (2.9)) so that the problem factorizes into two “Hydrogen atoms”. The subleading $1/N$ corrections can be treated perturbatively. That is the same situation of a nucleus with large charge $Ze \gg e$ surrounded by just two electrons.

Type-II tetraquarks. Let us consider now the (+) branch where the potential $V_{\text{eff,BO}}^+ = \frac{\Delta(R)}{N}$ is repulsive at small R and has a minimum at $R \sim a_{\bar{3}}$. We refer to the bound states that can possibly arise around the minimum as type-II tetraquarks. For such states, the Schrödinger

²For $SU(3)$, the antisymmetric representation coincides with the antifundamental, so that the unique color singlet contraction of the diquark and the two antiquarks is the same as that of a baryon.

equation for the R coordinate is approximately that of a one-dimensional harmonic oscillator, with frequency $\omega \sim \sqrt{\frac{E_0}{Na_3^2 M_2}} \sim \sqrt{\frac{Nm_3}{M_2} \frac{E_0}{N}}$ set by the BO potential.³ The low-lying bound states of such a harmonic oscillator are localized within a length $\Delta R \sim \left(\frac{Nm_3}{M_2}\right)^{1/4} a_3$ from the minimum of the potential. The choice $\frac{Nm_3}{M_2} \ll 1$, then coincidentally implies the BO condition of eq. (3.10) and the validity of the harmonic oscillator approximation for the BO potential around the minimum. That allows to self-consistently identify a set of bound states, with energies given by

$$E_{\text{type-II}} = E_0 - \mathcal{O}\left(\frac{\mathcal{E}_3}{N}\right) + \mathcal{O}(\omega), \tag{3.19}$$

below the two-meson thresholds. In figure 7, we show a sketch of the type-II tetraquarks. In contrast to the type-I states, the type-II tetraquarks correspond to a highly entangled superposition in color and coordinate space. In other words they are not in a definite color configuration.

Note that the BO potentials shown in figure 5 are not only suppressed by $1/N$ but have an additional numerical $\mathcal{O}(0.1)$ suppression at the minimum, leading to tetraquarks that are very close to the two meson threshold. Remarkably, this numerical suppression can be shown to happen generically and is easily understood given the potential in equation (3.16) obtained for $m_3 \gg m_4$. To make the discussion more clear, consider potentials of similar form

$$V_\epsilon(X) = e^{-X} \left(\frac{1}{X} - \epsilon X \right), \tag{3.20}$$

where we introduced an additional parameter ϵ . The minimum of this potential occurs at $X_{\min} \sim 1/\sqrt{\epsilon}$, where it is of order $\sqrt{\epsilon} e^{-1/\sqrt{\epsilon}}$. Hence an *algebraically* small ϵ leads to an *exponentially* suppressed energy difference between the tetraquarks and the threshold.⁴ Even for $\epsilon = 2/3$ as in eq. (3.16), the position of the minimum is already at a somewhat large value of $X \simeq 2.07$, leading to a significant suppression from the exponential. Similarly for $m_3 \sim m_4$, the potential has an overall exponential factor coming from the wavefunction overlap, which again leads to an exponential suppression if the minimum occurs at a large R/a_3 .

We have just seen that the condition $M_2 \gg Nm_3$ allows to identify two different types of tetraquarks, for which we could check a posteriori the validity of the BO approximation (see discussion around equation (B.9)). We can now ask more generally if that condition is indeed necessary for the existence of bound states in the BO effective potential. For the case of a particle with mass M in a central potential $V(r)$ such that $V(r)$ is zero at infinity, the following Bargmann-Schwinger condition [47, 48] is *necessary* for the existence of bound states

$$\int_0^\infty \Theta(-V(r)) r |V(r)| dr \geq \frac{1}{2M}, \tag{3.21}$$

³For non-zero and $\mathcal{O}(1)$ angular momentum l , the contribution of the “centrifugal” term is small compared to that of the BO potential around its minimum for $M_2 \gg m_3 N$. Hence its effect on the wavefunction for the coordinate R can be neglected. In other words the level separation due to rotational modes is small compared to the vibrational modes of the heavier quarks.

⁴A similar mechanism ensures the exponential suppression of mass scales generated by the slow RG evolution of marginally relevant parameters, like the gauge coupling in QCD or like the Goldberger-Wise dual coupling in the Randall-Sundrum model.

where the Heaviside theta function is inserted such that the integral is only over the regions where the potential is negative. The condition for the case of our BO potentials reads parametrically as $M_2 \gtrsim Nm_3$. That means that, without a hierarchy of masses (at least) as large as N , there are no four-quark bound states within the BO approximation.

Indeed by studying numerically the Schrödinger equation for our BO potentials, we found the critical ratio $\frac{M_{12}}{Nm_3}$ for which ground state tetraquarks are formed, where $M_{12} = \frac{M_1 M_2}{M_1 + M_2}$. In the limit $m_3 \gg m_4$, the critical ratio is 1.7 and 0.9 for respectively Type-I and Type-II tetraquarks. Instead for $m_3 = m_4$ we find somewhat larger critical ratios of 2.4 and 1.5 again for respectively Type-I and Type-II. We note that for parameters around the critical ratios the heavy quarks are not localized in a region $\Delta R \ll a_3$ and thus cannot be self-consistently described by the BO approximation. However, as we will see in section 4, for $m_3 = O(m_4)$, the bound state problem can be easily be studied beyond the domain of validity of the BO approximation. It also turns out that for the specific case $m_3 = m_4$, the BO approximation and the full treatment coincide at leading order in $1/N$ and m/M (see eq. (4.18)). Therefore, in this specific case, the critical ratios quoted above can be trusted even though they occur at the edge of validity of the BO approximation.

The very special case of very excited states. The study of tetraquarks within the BO approximation so far only considered light quarks sitting in their ground state. As discussed in the next section, particle statistics can force some of them to occupy an excited orbital. The condition of applicability of the BO approximation for the lowest excited states is of course still given by eq. (3.11). However, one may wonder what happens in the case of very excited orbitals, characterized by principal quantum numbers $n, n' \gg 1$. In order to get an idea we have repeated the analysis of this section for the case of large $n = n'$. What essentially happens is that the length scale of the BO potential now grows with n . In particular for type I tetraquarks, the region where the potential behaves like a Coulombic $\propto 1/R$, before having significant overlap suppression extends up $R \sim n^{3/2}a_3$. This can be understood as follows: for very small R , the overlap is dominated by the last peak of the meson wavefunction located at a distance $\sim n^2 a_3$. This peak has however a width of order $n^{3/2}a_3$ and therefore beyond the distance specified by the width, the BO potentials drops significantly compared to a $\propto 1/R$ Coulombic potential. We have confirmed this also numerically. At face value this implies bound states exist in a wider range of M ,

$$M > Nm_3/n^{3/2}. \tag{3.22}$$

On the other hand, the request of the BO condition eq. (3.10) implies a slightly tighter constraint

$$M > Nm_3/n, \tag{3.23}$$

which is nonetheless weaker than eq. (3.11). These constituent excited states are in reality expected to be unstable, as we do not see any conserved quantum number preventing their decay to either more deeply bound tetraquarks, through gluon emission, or to unbound mesons, possibly without gluon emission. So we are not sure how much significance to attribute to this result. Finally, considering the type II sector at large n one does not find any extension to the range of validity of the BO approximation.

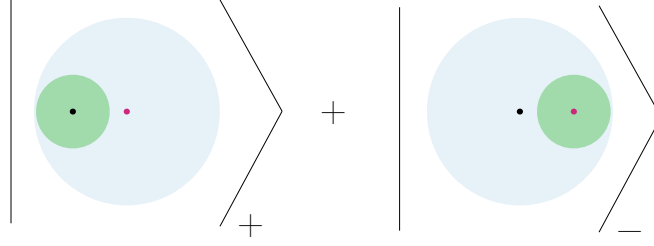


Figure 7. Sketch of the type-II tetraquarks. The black and red dots represent the heavier quarks and the colored regions are where the wavefunction of the lighter antiquarks have a significant support. The “+” and “-” subscripts denote the color configuration of the state, as defined in eq. (2.5). This state has no similarity to any state with a fixed color configuration.

3.4 Tetraquarks with identical quarks: spin-statistics and excited states

In this subsection we consider the cases with at least two identical quarks (or antiquarks). For non-identical quarks, all the states constructed so far are allowed, but in the presence of identical particles only the subset with the suitable transformation properties under permutations is allowed. A general state is described by a vector wave function $\Psi_{\alpha_1, \dots, \alpha_4, \beta}(\vec{r}_1, \vec{r}_2, \vec{r}_3, \vec{r}_4)$ with α_i labelling the spin of each quark and with $\beta = \pm$ labelling the two possible color singlet contractions associated with $P(\pm)_{mn}^{ij}$ (see eq. (2.10)). The constraints from statistics are expressed in terms of the action of the permutation operators, P_{12} and P_{34} , for respectively the quantum numbers of $Q_{1,2}$ and $\bar{q}_{3,4}$. Notice that under the permutation of the color indices of either $Q_{1,2}$ or $\bar{q}_{3,4}$ the color structures $P(\pm)_{mn}^{ij}$ are mapped into each other. The action of P_{12} on $\Psi_{\alpha_1, \dots, \alpha_4, \beta}(\vec{r}_1, \vec{r}_2, \vec{r}_3, \vec{r}_4)$ then consists in $\alpha_1 \leftrightarrow \alpha_2$, $\beta \rightarrow -\beta$, $\vec{r}_1 \leftrightarrow \vec{r}_2$. For P_{34} one has instead $\alpha_3 \leftrightarrow \alpha_4$, $\beta \rightarrow -\beta$, $\vec{r}_3 \leftrightarrow \vec{r}_4$.

Using the coordinate basis introduced at the beginning of section 3, in the BO approximation it is convenient to pick a basis of factorized wave functions of the form

$$\chi_{\alpha_1, \alpha_2, \alpha_3, \alpha_4}^{\text{spin}} \Phi_{\vec{P}_{CM}}(\vec{R}_{CM}) \Phi_{\tilde{n}\tilde{l}\tilde{m}}^{\mathcal{A}}(\vec{R}) \psi_{\beta}^{\mathcal{A}}(\vec{r}'_3, \vec{r}'_4; \vec{R}). \quad (3.24)$$

Here the first factor χ^{spin} is a coordinate independent vector in spin space. The second describes the motion of the CM and plays no role in our discussion of bound states. The third factor describes a state of the Q_1 - Q_2 system with orbital quantum number \tilde{n} and angular momentum numbers \tilde{l}, \tilde{m} .⁵ The last factor is the wavefunction for the color (index β) and for the coordinates of the lighter antiquarks, which as we have seen can be entangled. The label “ \mathcal{A} ”, which is common to the last two factors, describes the overall color configuration and the orbital configuration of $\bar{q}_{3,4}$. Hence it also labels the resulting BO potential and orbital states of the Q_1 - Q_2 system.

Let us consider first the case of identical $\bar{q}_{3,4}$. As it turns out, it will in some case be necessary to consider excited states of the reduced \bar{q}_3 - \bar{q}_4 Hamiltonian. We must thus proceed with slightly more generality than in the previous sections, by identifying the symmetries of the reduced Hamiltonian and by characterizing the \mathcal{A} quantum numbers.

⁵Notice that, as the effective BO Hamiltonian in eq. (3.9) is rotationally invariant, it’s eigenstates can be chosen to have definite angular momentum.

To identify the symmetries of the reduced Hamiltonian, where \vec{R} is treated as a parameter, we should first identify the symmetries of the full Hamiltonian with the kinetic terms of the heavy quarks neglected. These are rotations (SO(3)), parity (Π), the full exchange of the light quark quantum numbers $P_{\bar{3}\bar{4}}$ (for $m_{\bar{3}} = m_{\bar{4}}$), but also that of the heavy quark quantum numbers P_{12} . The latter is not a symmetry of the full Hamiltonian for $M_1 \neq M_2$, but the neglect of the kinetic terms restores it. The symmetry of the reduced Hamiltonian is then the subgroup of the above symmetries under which the position vector \vec{R} is left invariant. Choosing coordinates such that \vec{R} is along the z axis we then have that the residual symmetries of the reduced Hamiltonian are:

- SO(2) rotations around the z axis: the states of the light antiquarks can then be labeled by the angular momentum in the z direction, m_z , and eigenstates of the leading Hamiltonian with different m_z are not mixed by the subleading terms of the Hamiltonian.
- Parity in the (x, y) -plane: $A_y : (x, y) \rightarrow (x, -y)$. Note that $A_y L_z = -L_z A_y$, corresponding to $\text{SO}(2) \times A_y = O(2)$. Then the action of A_y on any state with $m_z \neq 0$ gives a corresponding degenerate state with equal and opposite m_z .
- The Z_2 transformation $\tilde{\Pi} = P_{12}\Pi$. Indeed, as $\vec{R} \rightarrow -\vec{R}$ under both P_{12} and Π , their combined action clearly leaves \vec{R} invariant. Indeed, thanks to eqs. (3.4), (3.5), $\tilde{\Pi}$ can also be written by combining the action of parity on the antiquarks $\bar{\Pi} : \vec{r}'_{\bar{3},\bar{4}} \rightarrow -\vec{r}'_{\bar{3},\bar{4}}$ with the exchange of their color indices. In the \pm color wave-function space that corresponds to

$$\tilde{\Pi} = \begin{pmatrix} 0 & \bar{\Pi} \\ \bar{\Pi} & 0 \end{pmatrix}. \quad (3.25)$$

Note that $\tilde{\Pi}$ commutes with both L_z and A_y .

- $P_{\bar{3}\bar{4}}$.

Let us now construct the complete labels \mathcal{A} of the light anti-quark states. In the leading $N \rightarrow \infty$ approximation the eigenstates of the reduced Hamiltonian, see eq. (3.12), are simply pairs of mesons. In an obvious notation, these can be labelled as

$$|\pm; \{n, l, m\}, \{n', l', m'\}\rangle \equiv |\mathcal{A}\rangle, \quad (3.26)$$

where, besides the color contraction \pm , the first set of quantum numbers specify the state of \bar{q}_3 , and the second set that of \bar{q}_4 . For these states, the coordinates \vec{r}'_3 and \vec{r}'_4 are centered respectively around $-\vec{R}/2$ and $\vec{R}/2$ for the $+$ color configuration (and instead around $\vec{R}/2$ and $-\vec{R}/2$ for the $-$ color configuration).

The action of L_z , A_y , $\tilde{\Pi}$ and $P_{\bar{3}\bar{4}}$ in this basis is given by⁶

$$L_z |\pm; \{n, l, m\}, \{n', l', m'\}\rangle = (m + m') |\pm; \{n, l, m\}, \{n', l', m'\}\rangle \quad (3.27)$$

$$A_y |\pm; \{n, l, m\}, \{n', l', m'\}\rangle = |\pm; \{n, l, -m\}, \{n', l', -m'\}\rangle \quad (3.28)$$

$$\tilde{\Pi} |\pm; \{n, l, m\}, \{n', l', m'\}\rangle = (-1)^{l+l'} |\mp; \{n, l, m\}, \{n', l', m'\}\rangle \quad (3.29)$$

$$P_{\bar{3}\bar{4}} |\pm; \{n, l, m\}, \{n', l', m'\}\rangle = |\mp; \{n', l', m'\}, \{n, l, m\}\rangle. \quad (3.30)$$

⁶The action of A_y corresponds to choosing the standard spherical harmonics for angular momentum eigenstates, which satisfy $Y_{l,m}(\theta, -\varphi) = Y_{l,-m}(\theta, \varphi)$.

We have now all the ingredients to construct the states for identical bosonic or fermionic $\bar{q}_3 \bar{q}_4$. Acting with the projectors $\frac{1}{2}(1 \pm P_{34})$ we project on states that are symmetric or antisymmetric under exchange the color and the position of \bar{q}_3 - \bar{q}_4

$$\text{anti-symmetric} \quad \frac{1}{2} [|+\rangle; \{n, l, m\}, \{n', l', m'\} \rangle - |-\rangle; \{n', l', m'\}, \{n, l, m\} \rangle] \quad (3.31)$$

$$\text{symmetric} \quad \frac{1}{2} [|+\rangle; \{n, l, m\}, \{n', l', m'\} \rangle + |-\rangle; \{n', l', m'\}, \{n, l, m\} \rangle]. \quad (3.32)$$

These states have to be combined with a spin wave-function with the suitable transformation under P_{34} . Notice that, according to the discussion in the previous sections, in the ground state $n = n' = 1$ and $l = m = l' = m' = 0$ the anti-symmetric and symmetric states correspond respectively to type I and type II tetraquarks. Then in the case of identical fermionic anti-quarks, the total spin of the $\bar{q}_3 - \bar{q}_4$ system should be 1 and 0 for respectively type-I and type-II tetraquarks.

If instead $\bar{q}_{3,4}$ are identical scalars, the absence of a spin factor leaves as the only option for their ground state the symmetric combination in eq. (3.32), corresponding to the type-II tetraquark $|\psi_0^+\rangle + |\psi_0^-\rangle$. However when considering excited states with $(n, l, m) \neq (n', l', m')$, also type-I tetraquarks are allowed by the statistics. In some situation these may even constitute the ground state of the full system, as can be seen even bypassing all the careful classification we have been making. Consider indeed the regime $M_2 \gg N^2 m_3$ where one can first solve for the $Q_1 - Q_2$ diquark bound state in the antisymmetric color configuration. The resulting binding energy dominates over all other contributions, in particular over the binding energies of the lighter antiquarks. One can then construct bound states of the diquark and of the two antiquarks which are symmetric under exchange of \bar{q}_3 and \bar{q}_4 and whose energy is obviously lower than that of the type-II state. Therefore for $M_2 \gg N^2 m_3$, the ground state is in this class.

To get an idea of the states that arise when considering excited antiquark orbitals, consider the simplest such case $\{n, n'\} = \{1, 2\}$. The symmetric subset of these states in eq. (3.32) has an eight-fold degeneracy at leading order in $1/N$: a factor 4 from the spin states of the $n = 2$ orbital and a factor 2 from color. Now, the operators $\frac{1}{2}(1 \pm \tilde{\Pi})$ project on 4-dimensional subspaces which do not mix even considering higher orders, given $\tilde{\Pi}$ is a symmetry. Each subspace features one state with $m_z = 1$, one with $m_z = -1$, and two states with $m_z = 0$. Invariance under $SO(2)$ forbids mixing between $m_z = 1$, or $m_z = -1$, with all the other states. Moreover, as A_y maps these states into each other, their energies (and the corresponding BO effective potential) are degenerate. Instead the two states with $m_z = 0$ in general mix. At any fixed R the BO potentials are then found by diagonalizing the $1/N$ perturbation in this two dimensional subspace. The result is shown in figure 8. Note that the corresponding states with opposite $\tilde{\Pi}$ quantum numbers lead to BO potentials with the same magnitude but opposite sign. This stems from the fact that the $1/N$ correction to the Hamiltonian is off-diagonal in the basis of eq. (2.7). The shape of these potential makes it evident that there exist both type I and type II tetraquarks even for identical bosonic $\bar{q}_{3,4}$ as soon as their excited orbital states are considered.

For identical heavier quarks $Q_{1,2}$, both type-I and type-II tetraquarks are allowed as the full action of the permutation P_{12} now also depends on the angular momentum quantum

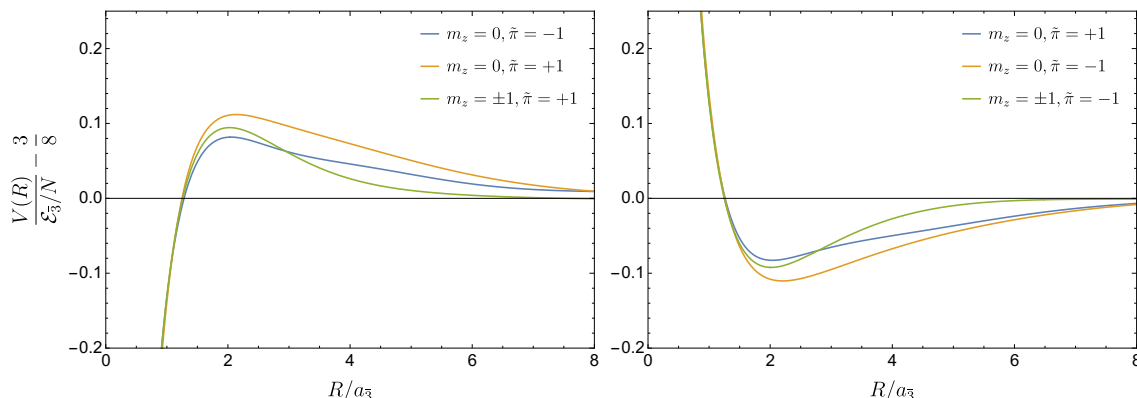


Figure 8. The first excited BO-potentials for identical antiquarks and $P_{\bar{3}\bar{4}}$ -symmetric wavefunctions. Left: BO potentials which lead to type-I tetraquarks. Right: BO potentials leading to type-II tetraquarks. $\tilde{\pi}$ denotes the eigenvalue of the $\tilde{\Pi}$ transformation. Note that the $m_z = \pm 1$ potentials are degenerate on both sides.

number \tilde{l} in eq. (3.24). Consider indeed for simplicity the ground state $n = n' = 1$ of the antiquark orbital. The action of P_{12} on the states in eqs. (3.31), (3.32) is just a flip of $+$ and $-$: type I ($|\psi_0^+\rangle - |\psi_0^-\rangle$) has then $P_{12} = -1$ while II ($|\psi_0^+\rangle + |\psi_0^-\rangle$) has $P_{12} = +$. These should be suitably combined with the action of P_{12} on the orbital part, $(-1)^{\tilde{l}}$, and on the spin part which for fermionic quarks is $(-1)^{S+1}$. Identical bosonic quarks and identical fermionic quarks in the $S = 0$ state then feature the same correlation between tetraquark type and angular momentum \tilde{l} : type-I eigenstates have odd \tilde{l} while type-II have even \tilde{l} . For fermionic quarks in the $S = 1$ spin state one has the reverse: type I have even \tilde{l} while type II have odd \tilde{l} .

4 Beyond Born-Oppenheimer

We will here study the $Q_1 Q_2 \bar{q}_3 \bar{q}_4$ ground state supplementing eq. (3.1) with

$$Nm_{\bar{3}} \gg M_2 \gg m_{\bar{3}}, \quad (4.1)$$

for which the Born-Oppenheimer approximation fails. Deriving an effective description for slow moving ground state meson system and applying variant of the Bargmann-Schwinger condition we will show that the ground state consists of two unbound mesons. Indeed our argument is also easily adapted to show that also for other mass hierarchies and other mass ordering the ground state consists of a meson pair. In particular we do so for the case of a heavy quark and heavy antiquark $Q_1 \bar{Q}_3 q_2 \bar{q}_4$ corresponding to $M_1 > M_{\bar{3}} > m_2 > m_{\bar{4}}$.

4.1 Two heavy quarks and two lighter anti-quarks

Recall that in the regime of eq. (3.11) where the BO approximation was applicable, we could ignore the kinetic terms of the heavier quarks when solving for the light anti-quark dynamics up to subleading $1/N$ order. The heavy quark dynamics was then solved in a second step. In the regime of eq. (4.1), which we are here considering, this is no longer possible: $Q_{1,2}$ are here not heavy enough to permit neglecting their recoil effect on the light anti-quark dynamics at order $1/N$. We must then swap the order at which we include $1/M$ and $1/N$

effects. For the present analysis, as it will be soon clarified, it is convenient to work in the singlet-adjoint (I/Ad) basis. The Hamiltonian takes the form

$$H = \frac{P_1^2}{2M_1} + \frac{P_2^2}{2M_2} + \frac{p_3^2}{2m_{\bar{3}}} + \frac{p_4^2}{2m_{\bar{4}}} + V^{(0)} + \frac{1}{N} V^{(1)} + \mathcal{O}\left(\frac{1}{N^2}\right), \quad (4.2)$$

where the leading order potential is

$$V^{(0)} = -\alpha \begin{pmatrix} \frac{1}{r_{1\bar{3}}} + \frac{1}{r_{2\bar{4}}} & 0 \\ 0 & \frac{1}{r_{1\bar{4}}} + \frac{1}{r_{2\bar{3}}} \end{pmatrix}, \quad (4.3)$$

and where the $1/N$ correction is purely off-diagonal with matrix elements

$$V_{I,\text{Ad}}^{(1)} = V_{\text{Ad},I}^{(1)} = \alpha \begin{pmatrix} \frac{1}{r_{12}} + \frac{1}{r_{\bar{3}\bar{4}}} & -\frac{1}{r_{1\bar{4}}} - \frac{1}{r_{2\bar{3}}} \\ -\frac{1}{r_{1\bar{4}}} - \frac{1}{r_{2\bar{3}}} & \frac{1}{r_{12}} + \frac{1}{r_{\bar{3}\bar{4}}} \end{pmatrix}. \quad (4.4)$$

The full potential in this basis is given in eq. (A.9). As we shall better explain below, the benefit of the singlet-adjoint basis is that the off-diagonal potential manifestly falls off faster than $1/R$ at large meson separation. The leading order system is exactly solvable and consists of two decoupled sectors each containing two non-interacting mesons (and their excited states). We call these sectors A and B , where A is the sector involving $Q_1\bar{q}_3$ and $Q_2\bar{q}_4$ mesons while B involves $Q_1\bar{q}_4$ and $Q_2\bar{q}_3$. To solve the problem, besides the common CM coordinate \vec{R}_{CM} , it is convenient to use different coordinate bases in sector A and sector B . In sector A we choose $\vec{r}_{1\bar{3}}$ and $\vec{r}_{2\bar{4}}$, which describe the inner dynamics of the $(1\bar{3})$ and $(2\bar{4})$ mesons, and the relative distance between their centers of mass

$$\vec{R}_A = \frac{M_1\vec{r}_1 + m_{\bar{3}}\vec{r}_{\bar{3}}}{M_1 + m_{\bar{3}}} - \frac{M_2\vec{r}_2 + m_{\bar{4}}\vec{r}_{\bar{4}}}{M_2 + m_{\bar{4}}}. \quad (4.5)$$

In sector B , in full analogy, we choose instead $\vec{r}_{1\bar{4}}$ and $\vec{r}_{2\bar{3}}$, as well as

$$\vec{R}_B = \frac{M_1\vec{r}_1 + m_{\bar{4}}\vec{r}_{\bar{4}}}{M_1 + m_{\bar{4}}} - \frac{M_2\vec{r}_2 + m_{\bar{3}}\vec{r}_{\bar{3}}}{M_2 + m_{\bar{3}}}. \quad (4.6)$$

We indicate the momenta conjugate to \vec{R}_A and \vec{R}_B as respectively \vec{P}_A and \vec{P}_B . The Hamiltonian then becomes

$$H = \frac{P_{CM}^2}{2(M_1 + M_2 + m_{\bar{3}} + m_{\bar{4}})} + \begin{pmatrix} \frac{P_A^2}{2\mu_A} + \frac{p_{1\bar{3}}^2}{2\mu_{1\bar{3}}} + \frac{p_{2\bar{4}}^2}{2\mu_{2\bar{4}}} & 0 \\ 0 & \frac{P_B^2}{2\mu_B} + \frac{p_{1\bar{4}}^2}{2\mu_{1\bar{4}}} + \frac{p_{2\bar{3}}^2}{2\mu_{2\bar{3}}} \end{pmatrix} + V, \quad (4.7)$$

where $\mu_{i\bar{j}} = \frac{M_i m_{\bar{j}}}{M_i + m_{\bar{j}}}$ are the reduced masses corresponding to relative coordinates $\vec{r}_{i\bar{j}}$ and $\mu_{A,B}$ are given by

$$\mu_A = \frac{(M_1 + m_{\bar{3}})(M_2 + m_{\bar{4}})}{M_1 + m_{\bar{3}} + M_2 + m_{\bar{4}}}, \quad \text{and} \quad \mu_B = \frac{(M_1 + m_{\bar{4}})(M_2 + m_{\bar{3}})}{M_1 + m_{\bar{4}} + M_2 + m_{\bar{3}}}. \quad (4.8)$$

According to eq. (3.1), the ground states energies in the A and B sector, which we indicate respectively by E_A and E_B , are separated by a positive energy gap

$$\Delta E \equiv E_B - E_A \simeq \frac{(M_1 - M_2)(m_{\bar{3}} - m_{\bar{4}})}{M_1 M_2} (\mathcal{E}_{\bar{3}} + \mathcal{E}_{\bar{4}}) \longrightarrow \frac{m_{\bar{3}}}{M_2} \mathcal{E}_{\bar{3}}. \quad (4.9)$$

In the last step we have taken for illustrative purpose the limit $M_1 \gg M_2$, $m_{\bar{3}} \gg m_{\bar{4}}$, but notice that the gap disappears if either the quarks or the antiquarks are degenerate. A sketch of the spectrum is shown in the left panel of figure 9.

The leading order Hamiltonian is diagonal in the basis $\{|A, \vec{P}_A, \alpha_A\rangle, |B, \vec{P}_B, \alpha_B\rangle\}$ where the $\alpha_{A,B}$ denote the quantum numbers of the hydrogen-like problem. As such, they can be either discrete, when they describe mesons states, or continuous.⁷ A general state of the system can be written as

$$|\Psi\rangle = \sum_{\alpha_A} \int d^3 R_A \psi_{\alpha_A}(\vec{R}_A) |A, \vec{R}_A, \alpha_A\rangle + \sum_{\alpha_B} \int d^3 R_B \psi_{\alpha_B}(\vec{R}_B) |B, \vec{R}_B, \alpha_B\rangle. \quad (4.10)$$

The problem is now to study under what condition the $1/N$ correction to the potential in eq. (4.4) is sufficiently strong a perturbation of the zeroth order Hamiltonian to lead to meson-meson bound states. In fact we can ask two different questions: one is whether the lowest energy state is a bound state, the other is whether there exist bound states composed of excited mesons. For this second class of states, as we already mentioned, we do not see any argument for absolute stability, so that we expect them to become metastable when including corrections to the BO approximations and/or when bringing dynamical gluons back into existence. We will study here only the first question, though we think our study could easily be extended to that case as well. We will prove, subject to a reasonable assumption about the spectrum of excited states, that the ground state of the system is a tetraquark only in the same range where the BO approximation applies, i.e. for $M_2 \gtrsim m_{\bar{3}} N$. We think with some more effort we could also prove our additional assumption thus making our argument complete. However we think that would take us way beyond the scope of this paper.

In order to proceed it is convenient to first shift the unperturbed N^0 Hamiltonian $H_0 \rightarrow H_0 - E_A \equiv H'_0$, so that the unperturbed ground state has zero energy. Then, as the perturbation $V^{(1)}/N$ vanishes for $R_{A,B} \rightarrow \infty$, the condition for the existence of a stable tetraquark is that the spectrum of the perturbed Hamiltonian $H' \equiv H'_0 + V^{(1)}/N$ extend to negative values. In order to assess that, we should study the expectation value of H' over the most general class of states in eq. (4.10). We will not perform this study in full generality but we will work under the reasonable assumption that the lowest energy state of the full Hamiltonian is dominantly a linear superposition of states in the low end of the unperturbed spectrum and study in detail the most general such states.⁸ Consider now the spectrum in figure 9. To simplify the discussion we will work under the assumption that the gap $E_B - E_A$ between the ground states is parametrically smaller than the gap $\mathcal{E}_{\bar{4}}$ to the first excited meson

⁷Notice that the portion of the excited meson spectrum, discrete or continuous, with absolute value of the energy $\lesssim \Lambda_{\text{QCD}}$ is not described by weakly coupled non-relativistic quantum mechanics. Still, as we will now argue, these states decouple from the study of the ground state problem. That is therefore not an issue.

⁸Notice that in the limit $N \rightarrow \infty$ with all other parameters fixed we expect perturbation theory to apply, in such a way that eigenvalues above a certain finite gap will remain positive under the perturbation.

state. For instance we can focus on the case $m_{\bar{3}} \sim m_{\bar{4}}$ which implies $\mathcal{E}_{\bar{3}} \sim \mathcal{E}_{\bar{4}}$ and hence $E_B - E_A \ll \mathcal{E}_{\bar{4}}$ according to eqs. (4.1) and (4.9).⁹ For this choice of parameters, we will then proceed as follows. We will divide the Hilbert space as the direct sum of two subspaces

$$\mathcal{H} = \mathcal{H}_{\text{GS}} \oplus \mathcal{H}_{\text{exc}}, \quad (4.11)$$

where \mathcal{H}_{GS} and \mathcal{H}_{exc} consists respectively of the unperturbed states with energy below and above the gap $\mathcal{E}_{\bar{4}}$ to the lowest excited meson state. Labelling by $|A, \vec{R}_A, GS\rangle$ and $|B, \vec{R}_B, GS\rangle$ the ground state meson states for sector A and B respectively, we then have that \mathcal{H}_{GS} is made up of the most general superposition

$$|\Psi\rangle = \int d^3 R_A \psi_A(\vec{R}_A) |A, \vec{R}_A, GS\rangle + \int d^3 R_B \psi_B(\vec{R}_B) |B, \vec{R}_B, GS\rangle, \quad (4.12)$$

subject to the constraint

$$\frac{P_A^2}{2\mu_A} + \frac{P_B^2}{2\mu_B} < \mathcal{E}_{\bar{4}}, \quad (4.13)$$

corresponding to momenta in the range

$$P_{A,B} \lesssim \sqrt{M_2 \mathcal{E}_{\bar{4}}} \sim \sqrt{\frac{M_2}{m_{\bar{4}}}} \frac{1}{a_{\bar{4}}}. \quad (4.14)$$

The complementary subspace \mathcal{H}_{exc} consist then, obviously, of states either involving at least one excited mesons or with kinetic energy exceeding $\mathcal{E}_{\bar{4}}$.

The idea is now that bound states, when they first appear as a function of the parameters, they will approximately consist of linear superposition of states in \mathcal{H}_{exc} . To study the problem we can then “integrate” out the states in \mathcal{H}_{exc} and derive an effective Hamiltonian for the reduced ground state Hilbert space \mathcal{H}_{GS} . This procedure is discussed in more detail in appendix D, but the basic implication is easily explained by thinking in terms of standard perturbation theory. As the states in \mathcal{H}_{GS} have a fixed gap, their contribution to the low energy effective Hamiltonian is quadratic in the perturbation $V^{(1)}/N$ and hence scales like $1/N^2$. This should be compared to the matrix elements of $V^{(1)}/N$ between states in \mathcal{H}_{GS} , which evidently only scale like $1/N$. This different scaling implies (as better detailed in the appendix) that the effects of the virtual excited states is always subdominant for the purpose of assessing the first occurrence of bound states. To study the latter one can then simply study the bound state problem in \mathcal{H}_{GS} with a Hamiltonian simply given by H' projected to \mathcal{H}_{GS} . The rest of this section is devoted to that.

We need to compute the matrix elements of $V^{(1)}$ on \mathcal{H}_{GS} . The potential can be written in our Hilbert space basis as $P_{AB} V_{I,Ad}^{(1)}(r_1 \dots r_4)$ where P_{AB} is the operator switching color contraction $A \leftrightarrow B$ and satisfying $P_{AB}^2 = \mathbb{I}$. For the overlap between the basis states we

⁹We do not expect our conclusions to be affected by this hypothesis. For instance, one could repeat the analysis of this section for the case of just three particles $Q_{1,2}$ and \bar{q}_3 , which corresponds to the formal limit $m_{\bar{4}} \rightarrow 0$ and for which the unperturbed spectrum consists of states involving one meson and one unbound heavy quark. One would reach the same conclusions.

then find¹⁰

$$\langle A, \vec{R}_A, GS | P_{AB} | B, \vec{R}_B, GS \rangle \sim \delta^3(\vec{R}_A - \vec{R}_B) e^{-R_A/a_3} e^{-R_A/a_4}, \quad (4.15)$$

which leads to

$$\langle A, \vec{R}_A, GS | V^{(1)} | B, \vec{R}_B, GS \rangle \simeq \Delta(R_A) \delta^3(\vec{R}_A - \vec{R}_B), \quad (4.16)$$

up to corrections that are controlled by m/M , where $\Delta(R)$ was defined in eq. (3.15). On \mathcal{H}_{GS} we can then write the energy functional as

$$\begin{aligned} \langle \Psi | H' | \Psi \rangle = & - \int d^3 R_A \psi_A^*(\vec{R}_A) \frac{\nabla^2}{2\mu_A} \psi_A(\vec{R}_A) + \int d^3 R_B \psi_B^*(\vec{R}_B) \left(-\frac{\nabla^2}{2\mu_B} + \Delta E \right) \psi_B(\vec{R}_B) \\ & \times \int d^3 R_A d^3 R_B \psi_A^*(\vec{R}_A) \psi_B(\vec{R}_B) \Delta(R_A) \delta^3(\vec{R}_A - \vec{R}_B) + \text{c.c.}, \end{aligned} \quad (4.17)$$

which leads to the Schrödinger equation

$$\left[- \begin{pmatrix} \frac{\nabla^2}{2\mu_B} & 0 \\ 0 & \frac{\nabla^2}{2\mu_B} \end{pmatrix} + \begin{pmatrix} \frac{\mu_A - \mu_B}{2\mu_A \mu_B} \nabla^2 & 0 \\ 0 & \Delta E \end{pmatrix} + \frac{\Delta(R)}{N} \begin{pmatrix} 0 & 1 \\ 1 & 0 \end{pmatrix} \right] \begin{pmatrix} \psi_A(\vec{R}) \\ \psi_B(\vec{R}) \end{pmatrix} = E \begin{pmatrix} \psi_A(\vec{R}) \\ \psi_B(\vec{R}) \end{pmatrix}. \quad (4.18)$$

The second term in square brackets is a positive semi-definite operator, as $\Delta E \geq 0$ and

$$\mu_B - \mu_A = \frac{(M_1 - M_2)(m_3 - m_4)}{M_1 + M_2 + m_3 + m_4} \geq 0. \quad (4.19)$$

Therefore, it can only increase the ground state energy. We will now study under what condition the modified Hamiltonian that results by dropping this term has a positive spectrum. A fortiori then, under the same condition also H' is positive definite, at least when reduced to the subspace of eq. (4.12).

The modified Hamiltonian is particularly simple and can be diagonalized by a basis rotation, $\psi_{A\pm B} = 1/\sqrt{2}(\psi_A \pm \psi_B)$. The system reduces to two decoupled subsectors with potentials $\pm \Delta(R)/N$. The application of the Bargmann-Schwinger condition of eq. (3.21) to these potential then shows that there are no bound states, i.e. the spectrum is positive, for the mass hierarchy $Nm_3 \gg M_2 \gg m_3$. This result is quickly understood. The function $\Delta(R)$ has the form $\mathcal{E}_3 F(R/a_3)$ in such a way that the integral at the left hand side of eq. (3.21) is of order $\mathcal{E}_3 a_3^2/N \sim 1/(Nm_3)$. As the right hand side is $\sim 1/M_2$, our result follows.

Finally we note that eq. (4.18) contains the BO approximation when specified to the regime $m/M \ll 1/N$, as in this regime the second term in the square bracket can be neglected. Furthermore, as we already noted in section 3.3, in the case of degenerate masses with either $m_3 = m_4$ or $M_1 = M_2$, the problem of finding the bound states using eq. (4.18) becomes identical to that within the BO approximation. Therefore, the critical value of $\frac{M_{12}}{Nm_3}$ above which stable tetraquarks exist, which we quoted in that section, can actually be trusted for identical masses even though that happens in the regime where m/M and $1/N$ are of the same order.

¹⁰Given that $\vec{R}_A = \vec{R}_B + \mathcal{O}(\frac{m}{M}\vec{R}_B) + \mathcal{O}(\frac{m}{M}\vec{r}_{ij})$, the wave function overlap in eq. (4.15) is exponentially suppressed unless $|\vec{R}_A - \vec{R}_B| \lesssim am/M$. As this length scale is smaller than implied by eq. (4.14), eq. (4.15) can be well approximated by a δ -function. Notice that our effective theory approach nicely ensures that the perturbation behaves like a potential between point particles.

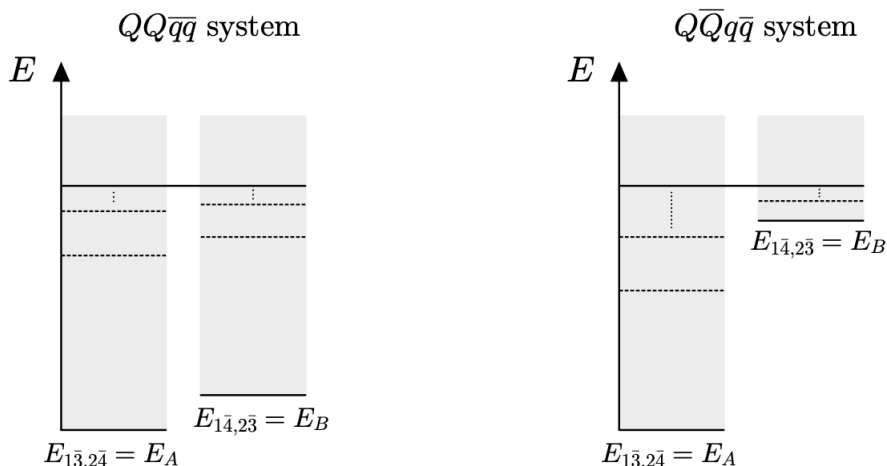


Figure 9. The typical spectrum of the two sectors considering only the interactions at leading order in $1/N$.

4.2 Alternative quark mass hierarchies and orderings

In the mass ordering considered in the previous section, the ground states in the A and B sectors could in principle have been very degenerate. In order to account for the possible compensation of the smallness of the $1/N$ perturbation by the small degeneracy we were then forced to consider an effective low energy description (the subspace \mathcal{H}_{GS}) which encompassed both sectors. We found that for the mass hierarchy of eq. (4.1) the ground state is not a tetraquark, essentially because the heavy quarks Q_1 and Q_2 in this regime are not heavy enough to make the $O(1/N)$ potential a large perturbation. This result suggest that we should be able to exclude stable tetraquarks also for the case where there is no hierarchy between M_2 and $m_{\bar{3}}$. Consider indeed the generic case where $M_1 > M_2 > M_3 > M_4$ with all masses roughly of order M . In this case the gap between the A and B ground states as well as that to first excited meson is $\sim \alpha^2 M$. Proceeding like in the previous section, the study of the effect of the $1/N$ suppressed terms can be carried out by zooming on the effective dynamics on a suitable low energy portion \mathcal{H}_{GS} of the Hilbert space. The natural choice is to have \mathcal{H}_{GS} cover the orbital states of the A sector ground state with energy below the relevant gap $\alpha^2 M$. The complement \mathcal{H}_{exc} contains then the whole B sector as well all the excited mesons plus the continuum in the A sector. The effective potential in the resulting effective description is then of order $1/N^2$ and comes from two sources. The first is the diagonal $1/N^2$ term in the original Hamiltonian. That is easily seen to trivially contribute to just a correction to the binding energy of the $1\bar{3}$ and $2\bar{4}$ mesons of the A sector, and thus does not influence the existence of stable tetraquarks. The second effect originates from integrating out the B sector, as discussed in the previous section and as detailed in appendix D. One can bound the size of this second contribution under the same reasonable hypothesis we applied previously, i.e. that the $O(\alpha^2 M)$ is not wildly modified by the perturbation. One then finds that the resulting effective potential roughly scales like $\sim (\alpha^2 M/N^2)f(RM\alpha)$ with f a fast decreasing function for $R \gg 1/(\alpha M)$ and non-singular at smaller R . With this result the integral on the left hand side of eq. (3.21) is roughly $O(1/(N^2 M))$. The criterion for the existence of meson bound states is not passed as soon as N is larger than $O(1)$.

In a similar manner we can investigate the $Q\bar{Q}q\bar{q}$ system corresponding to the mass ordering $M_1 \geq M_3 > M_2 \geq M_4$. That includes in particular the hierarchical case $M_1 \sim M_3 = O(M) \gg M_2 \sim M_4 = O(m)$ and the case where all masses are comparable and $O(M)$.¹¹ As the results are the same let us consider for definiteness the hierarchical case.

In the $N \rightarrow \infty$ limit this system again consists of two decoupled sectors of two non interacting meson states. Again, like in the case we just considered, there is a large gap between the ground states of the two towers (see the right panel of figure 9). In one sector, say A , the two mesons correspond to the pairing $(Q\bar{Q})$ and $(q\bar{q})$. The binding energy is dominated by that of the first couple and is of order $\alpha^2 M$. The mesons of the second sector, say B , are instead of the form $(Q\bar{q})$ and $(\bar{Q}q)$ with a much smaller binding energy of order $\alpha^2 m$. Again we can zoom on a low energy effective description limited to ground state meson states in the A sector, with kinetic energy below the $\sim \alpha^2 M$ gap. Like previously, the effective potential arises at $O(1/N^2)$ and consists of two contributions. A direct one, which trivially only provides a small correction to the $Q\bar{Q}$ and $q\bar{q}$ meson binding energy, and an indirect one arising from integrating out the B sector. Using analogous estimates as in appendix D, we find that this second contribution scales roughly like $(\alpha^2 m/N^2)(m/M)^3 f(R\alpha m)$, with f smooth at short distances and rapidly decreasing for $R \gg 1/(\alpha m)$. For such potential the integral on the left hand side of eq. (3.21) is roughly $(1/N^2)(m/M)^3 1/m$ which cannot even marginally beat the $1/m$ necessary for the occurrence of a bound state. The case of comparable masses is simply obtained by taking $m \sim M$. The situation here coincides with the case first studied in this section: bound states are not possible as soon as N is bigger than $O(1)$.

We thus conclude that also for these other mass patterns the ground state consists of two mesons.

5 Discussion and speculations about real-world tetraquarks

Our study focused on the limit where N is large and all masses are far above Λ_{QCD} . Note however, as already pointed out in section 3, all our results are basically unaffected even in the case $m_4 \lesssim \Lambda_{\text{QCD}}$, as long as $m_3 \gg \Lambda_{\text{QCD}}$ remains satisfied. Indeed in that case the effects of \bar{q}_4 in the binding dynamics are negligible, with type I and type II tetraquarks bound by the larger binding energies associated with the three heavier quarks Q_1, Q_2, \bar{q}_3 . Notice that for this range of masses the excitation spectrum associated with the \bar{q}_4 orbitals, and characterized by energy splittings of order Λ_{QCD} , is now beyond perturbative control. The larger splittings associated with the heavier quarks remain however under control. The properties of the states with excited \bar{q}_3 orbitals are the same as discussed in section 3. In particular for $N^2 \gg M_2/m_3 \gg N$ these states are metastable with respect to decay into the ground state mesons.

The existence and the properties of type I tetraquarks are also largely unaffected by further taking m_3 below Λ_{QCD} , at least for the states where $Q_1 - Q_2$ attraction dominates

¹¹In the case where the flavors of a quark and an antiquark are identical, one could wonder if their annihilation may be important. However, this case also falls within our approximation. This is because the annihilation lifetime is parametrically longer than the other relevant time scales, as can be shown by inspecting the various time scales. For instance the annihilation width for a $\bar{Q}Q$ bound state with identical flavors is $\mathcal{O}(\alpha^5 M)$ or smaller, while its binding energy is $\mathcal{O}(\alpha^2 M)$.

the binding. That is easily seen to correspond to states where $R \ll \Lambda_{\text{QCD}}^{-1}$, which is realized for $M_2 \gg N\Lambda_{\text{QCD}}$. The resulting states belong to the same class of the hadrons with QQ content identified long ago in ref. [31]. On the other hand, for $\Lambda_{\text{QCD}} > m_3 \geq m_4$ the existence of type II tetraquarks depends on the detailed form of the BO potential induced at distances of order $\Lambda_{\text{QCD}}^{-1}$ by non-perturbative effects. Whether at small or large N the computation of this quantity can only be done within lattice QCD.

In this section we will try to qualitatively apply the picture obtained in our study to real world QCD. In that regard, we extrapolate our large N and large mass results to $N = 3$ and to the physical masses of b and c quarks. Although there are sizeable corrections, we expect that the qualitative picture is preserved, at least partially.

First we consider the case where all quark masses are above Λ_{QCD} with a “hierarchy” between quarks and antiquark masses. That is relevant for $bb\bar{c}\bar{c}$ states. As it was discussed in section 3.3, we expect stable tetraquark states to form for $\frac{M}{Nm}$ above some critical $\mathcal{O}(1)$ value, which we obtained for various BO potentials. Incidentally, in the real world the ratio $\frac{m_b}{Nm_c}$ is close to unity, making it hard to draw any robust conclusions. Taking the critical mass ratios obtained, $\frac{m_b}{Nm_c} > 4.8$ for Type-I and $\frac{m_b}{Nm_c} > 3$ for Type-II, at face value, we should not expect to see $bb\bar{c}\bar{c}$ tetraquarks that are stable with respect to strong decays into mesons. Of course we are well aware of the stunt represented by our extrapolation. Notice also, as we discussed at the end of section 3.3, the existence of excited tetraquark sitting above the two meson threshold has a lower critical ratio $\frac{M}{Nm}$. Of course the size of these excited mesons, given the closeness of m_c becomes quickly of order $\Lambda_{\text{QCD}}^{-1}$. Also for that reason we have not done a detailed study of the critical ratio for these excited states. Nonetheless by a rough rule of thumb (see eq. (3.22)), we expect the critical ratio $\frac{M}{Nm}$ for the existence of the first excited tetraquark to be roughly a factor $2^{-3/2} \sim 1/3$ smaller than the values quoted above. That is close to unity, which we take as indication that metastable $bb\bar{c}\bar{c}$ tetraquarks may well exist.

Next we consider the case where one anti-quark is light, $m_4 < \Lambda_{\text{QCD}}$. For the case of real world QCD, we may use the results of this regime for the case of $bb\bar{c}\bar{q}$ states, with \bar{q} being a light anti-quark (\bar{u} , \bar{d} , or \bar{s}). In this case, the BO potential is largely unaffected by the lightest anti-quark \bar{q} , corresponding to the regime $m_3 \gg m_4$. The critical mass ratio in this case is lower than the case $m_4 = m_3$. Again for ground state mesons, we find $\frac{m_b}{Nm_c} > 3.4$ for type-I and $\frac{m_b}{Nm_c} > 1.8$ for type-II, making the existence of these states more likely than $bb\bar{c}\bar{c}$. That is even more the case for the tetraquarks with excited c -quark orbital, for which the critical ratio is further reduced.

Let us finally consider the case of two light anti-quarks below the QCD scale, i.e. the possible $bb\bar{q}\bar{q}$ (T_{bb}), $bc\bar{q}\bar{q}$ (T_{bc}), and $cc\bar{q}\bar{q}$ (T_{cc}) states. In the heavy quark limit, the existence of the type-I states relies only on the short distance region where the BO potential is dominated by the Coulombic potential among the two heavy quarks. According to our results stable tetraquarks should then exist for $M_2 \gg N\Lambda_{\text{QCD}}$. Taken at face value for the real world, this result indicates that stable T_{bb} likely exist, while T_{bc} and T_{cc} lie at the edge. That is qualitatively in agreement with the recent observation of T_{cc} right around the two DD threshold [6]. Notice also that in the regime $M_2 \gg N\Lambda_{\text{QCD}}$ the binding energy of the heavy quarks dominates the $O(\Lambda_{\text{QCD}})$ contributions from the light quarks, whether in their ground state or whether in an excited state. The excited tetraquarks then can only cascade

decay to the ground state tetraquark through gluon emission (with consequent conversion into light mesons).

T_{bb} , T_{bc} and T_{cc} , in their type-I incarnation, correspond to the hadrons with QQ diquark core identified in ref. [31] and forming the subject of the studies in refs. [11, 12]. In these papers the masses of this family of tetraquarks was predicted on the basis of HQET in conjunction with quark-diquark symmetry and using the data for heavy-light mesons and heavy-light-light baryons. It is interesting to compare the results of these more systematic studies to the qualitative perspective we just offered above. In the case of T_{cc} , both analyses find that it lies well above the two meson threshold, in contrast with the experimentally determined value of its mass [6], which happens instead to agree with the in principle more rudimentary estimate based on the quark model in ref. [36]. Notice however that both analyses did not account for the finite size of the diquark which, as estimated in [37], could easily give a correction that is comparable to the mismatch with observation. The same corrections can equally be important for T_{bc} . In the case of T_{bb} , however, not only the predictions [11, 12, 36] for its mass are significantly below threshold but also finite size effects are reduced, by roughly a $(m_c/m_b)^2 \sim 10$ factor. According to these HQET + diquark symmetry a T_{bb} stable under QCD interaction should then definitely exist. In fact, lattice studies, see e.g. [49–51], have reached similar conclusions. This all appears in agreement with the more qualitative picture suggested by extrapolating the results of our study.

And what about the possibility for type II T_{bb} , T_{bc} , T_{cc} tetraquarks? As we already explained, unlike for type I states, their existence is not guaranteed in the realistic case of light anti-quarks below the QCD scale. It would hinge instead on the properties of the BO potential which we can only imagine computing through lattice QCD simulations. In fact, the current determination of the potential is not very precise at large separations, and it is unclear if an additional minimum at such separations exists [49]. But if a second minimum were determined to exist that would establish the existence of type-II tetraquarks in the T_{QQ} family. Lacking at the moment such precisely determination, we cannot nonetheless refrain from speculating about this possibility. By accepting it, we would then have two options, type I and type II, for the recently discovered T_{cc} , as both can accommodate the inferred quantum numbers. In the case of future discovery of T_{bb} (and T_{bc}) tetraquarks their types may be distinguished by their binding energy. While type-I tetraquarks get more and more bound for heavier constituents, the binding energy for type-II tetraquarks saturates at the minimum of the BO potential. Assuming T_{cc} is a type-I tetraquark, the corresponding T_{bc} would be more bound by order $\alpha^2 m_c/N^2 \sim \alpha_s^2 m_c$, while the corresponding T_{bb} state would have a binding energy of order $\alpha^2 m_b/N^2 \sim \alpha_s^2 m_b$. On the other hand, in the case of type-II, T_{bb} , T_{bc} , T_{cc} the binding energies should roughly be the same, as they become mass independent in the limit of infinite heavy quark mass. Moreover, besides the $1/N$ suppression of this energy which should survive in the realistic case, in our study we also find an additional accidental $O(1/10)$, due to the exponential behaviour of the light quark wave function. We have no robust reason for that, but if this accidental suppression were to also survive in the realistic case, then it would significantly help bringing the expected $O(\Lambda_{\text{QCD}})$ range of the binding energy of T_{cc} , closer to its observed $\sim 0.5 \text{ MeV}$ value.

In our construction of tetraquarks within the BO approximation we focused on $QQ\bar{q}\bar{q}$ states. The study of this case is simpler compared to that of $Q\bar{Q}q\bar{q}$ tetraquarks, even within the $1/N$ expansion. That is because at leading order in $1/N$ and in the large mass expansion, the two ground states of the reduced Hamiltonian eq. (3.7) are degenerate. Then, as discussed in section 4, the bound state problem can be studied by accounting for the subleading effects in a truncated low energy Hilbert space around the ground states. In the case of a heavy $Q\bar{Q}$ pair, however, the two different color contractions lead to very different binding energies. As we argued in section 4 the low energy effective description consists on just one sector, that involving the deeply bound $Q\bar{Q}$ meson. It is easy to see that at large N no tetraquarks bound states can form in this sector. However, our methodology does not allow us to explore, and thus construct or rule out, metastable $Q\bar{Q}q\bar{q}$ tetraquarks. Indeed the problem of finding the BO potentials as a function of the distance between the heavy $Q\bar{Q}$, even though more challenging, is well defined and we leave it for future work. It is interesting to determine whether these potentials admit minima at distances of the order of the size of the $Q\bar{q}$ mesons in which case metastable tetraquarks can form for sufficiently heavy masses of the heavier Q and \bar{Q} . This picture would be in line with the current observed candidate states which are all around the $Q\bar{q}$ meson pair thresholds and can decay to the more bound $(Q\bar{Q}, q\bar{q})$ pair of mesons.

Acknowledgments

We would like to thank Sergei Dubovsky, Glennys Farrar, Brian Henning, David Kaplan, Matthew Walters, Marek Karliner, Antonio Polosa, Angelo Esposito, Ivan Polyakov, Abhishek Mohapatra and Marc Wagner for discussions. This work is partially supported by the Swiss National Science Foundation under contract 200020-213104. RR and SS acknowledge the hospitality of the Perimeter Institute for Theoretical Physics and RR acknowledges support from the Simons Collaboration on Confinement and QCD Strings. ME and SS acknowledge the hospitality of the CERN theory group and SS acknowledges the hospitality of the Center for Cosmology and Particle Physics at NYU.

A Wave functions and the Hamiltonian

For the reader's ease, in this appendix, we describe the general structure of the states of a $qq\bar{q}\bar{q}$ system and write down the Hamiltonian in the different bases used in the main text.

A.1 The states of a $qq\bar{q}\bar{q}$ system

A complete set of quantum numbers of a single (anti-)quark state is given by: the position x , the color, the spin, and, when needed, additional internal degrees of freedom such as the flavor. The most general $q_1q_2\bar{q}_3\bar{q}_4$ state can thus be written as

$$|\Psi\rangle = \sum_{\rho} \int \prod_{k=1}^4 d^3x_k \Psi_{m_n}^{i_j}(x, \rho) |1_i(x_1, \rho_1) 2_j(x_2, \rho_2) \bar{3}^m(x_3, \rho_3) \bar{4}^n(x_4, \rho_4)\rangle. \quad (\text{A.1})$$

We collectively denoted the spin and the other internal quantum numbers of the k -th particle with the index ρ_k . The sum over the color indices is left implicit. The normalization of

the ket is chosen so that

$$\langle \Phi | \Psi \rangle = \sum_{\rho} \int \prod_{k=1}^4 d^3 x_k \Phi_{ij}^{*mn}(x, \rho) \Psi_{mn}^{ij}(x, \rho). \quad (\text{A.2})$$

As explained in the main text, we are only interested in the two-dimensional subspace of color singlet states. A class of basis can be defined by asking one pair of particles, either qq or $q\bar{q}$, to sit in a definite color representation (\mathcal{R}). Indeed, the second pair must always sit in the conjugate representation to neutralize the color. The wave function can then be expanded as

$$\Psi_{mn}^{ij}(x, \rho) = \sum_{\mathcal{R}} \Psi_{\mathcal{R}}(x, \rho) P(\mathcal{R})_{mn}^{ij} \quad (\text{A.3})$$

There are three possible bases of this kind corresponding to three possible pairings: (12) , $(1\bar{3}), (1\bar{4})$. In the first case, \mathcal{R} can be either the symmetric (S) or the anti-symmetric (A) representation while in the others \mathcal{R} is either the singlet (1) or the adjoint (Adj) representation. The normalized color wave functions are then given by

$$\begin{aligned} P(S)_{mn}^{ij} &= \frac{1}{\sqrt{2N(N+1)}} (\delta_m^i \delta_n^j + \delta_n^i \delta_m^j), & P(A)_{mn}^{ij} &= \frac{1}{\sqrt{2N(N-1)}} (\delta_m^i \delta_n^j - \delta_n^i \delta_m^j), \\ P(1_{1\bar{3}})_{mn}^{ij} &= \frac{1}{N} \delta_m^i \delta_n^j, & P(\text{Adj}_{1\bar{3}})_{mn}^{ij} &= \frac{1}{\sqrt{N^2-1}} \left(\delta_n^i \delta_m^j - \frac{1}{N} \delta_m^i \delta_n^j \right), \\ P(1_{1\bar{4}})_{mn}^{ij} &= \frac{1}{N} \delta_m^i \delta_n^j, & P(\text{Adj}_{1\bar{4}})_{mn}^{ij} &= \frac{1}{\sqrt{N^2-1}} \left(\delta_m^i \delta_n^j - \frac{1}{N} \delta_m^i \delta_n^j \right). \end{aligned} \quad (\text{A.4})$$

Each line corresponds to an orthonormalized basis. Note that the wave function for the adjoint state of the $(1\bar{3})$ ($(1\bar{4})$) pair agrees with the $(1\bar{4})$ ($(1\bar{3})$) singlet to leading order in N . Finally, let us note that the angle between two color states is given by

$$\cos \theta(\mathcal{R}_1, \mathcal{R}_2) = P(\mathcal{R}_1)_{ij}^{*mn} P(\mathcal{R}_2)_{mn}^{ij} \quad (\text{A.5})$$

and can be used to perform the change of basis.

A.2 The potential in different bases

Depending on the regime of the masses of the quarks and antiquarks, the $qq\bar{q}\bar{q}$ system is more easily studied using one particular choice of basis. Here, we collect the different alternatives used in the main text. The general form of the potential is the one in equation (2.3). Contracting the color structures with the wave functions previously introduced, we can extract the different matrix elements of the potential in the color singlet subspace. Using a notation where the generators in the full color space are denoted as $T_1^a = T^a \otimes \mathbb{I} \otimes \mathbb{I} \otimes \mathbb{I}$, we have

$$V_{\mathcal{R}_1, \mathcal{R}_2} = \alpha_s \sum_{i < j} \frac{\lambda_{ij}(\mathcal{R}_1, \mathcal{R}_2)}{r_{ij}}, \quad (\text{A.6})$$

with

$$\lambda_{ij}(\mathcal{R}_1, \mathcal{R}_2) = P^*(\mathcal{R}_1)_{mn}^{pq} \left(T_{(i)}^a T_{(j)}^a \right)_{pqkl}^{mnrs} P(\mathcal{R}_2)_{rs}^{kl}, \quad (\text{A.7})$$

where $P(\mathcal{R})$ is given in eq. (A.4) for the different representations.

Symmetric/anti-symmetric basis. When the states are chosen so that the two quarks sit in a definite color representation, either the symmetric or the anti-symmetric, the potential is

$$\begin{aligned}
 V_{SS} &= -\alpha_s \frac{(N+2)(N-1)}{4N} \left(\frac{1}{r_{1\bar{3}}} + \frac{1}{r_{2\bar{4}}} + \frac{1}{r_{2\bar{3}}} + \frac{1}{r_{1\bar{4}}} \right) + \alpha_s \frac{N-1}{2N} \left(\frac{1}{r_{12}} + \frac{1}{r_{\bar{3}\bar{4}}} \right), \\
 V_{SA} &= V_{AS} = -\alpha_s \frac{\sqrt{N^2-1}}{4} \left(\frac{1}{r_{1\bar{3}}} + \frac{1}{r_{2\bar{4}}} - \frac{1}{r_{2\bar{3}}} - \frac{1}{r_{1\bar{4}}} \right), \\
 V_{AA} &= -\alpha_s \frac{(N-2)(N+1)}{4N} \left(\frac{1}{r_{1\bar{3}}} + \frac{1}{r_{2\bar{4}}} + \frac{1}{r_{2\bar{3}}} + \frac{1}{r_{1\bar{4}}} \right) - \alpha_s \frac{N+1}{2N} \left(\frac{1}{r_{12}} + \frac{1}{r_{\bar{3}\bar{4}}} \right).
 \end{aligned} \tag{A.8}$$

Singlet/adjoint basis. In the basis where the color state of the pair ($1\bar{3}$) is either in the singlet or in the adjoint representation we have the potential

$$\begin{aligned}
 V_{II} &= -\alpha_s \frac{N^2-1}{2N} \left(\frac{1}{r_{1\bar{3}}} + \frac{1}{r_{2\bar{4}}} \right), \\
 V_{IAd} &= V_{AdI} = -\alpha_s \frac{\sqrt{N^2-1}}{2N} \left(\frac{1}{r_{1\bar{4}}} + \frac{1}{r_{2\bar{3}}} - \frac{1}{r_{12}} - \frac{1}{r_{\bar{3}\bar{4}}} \right), \\
 V_{AdAd} &= -\alpha_s \frac{N^2-2}{2N} \left(\frac{1}{r_{1\bar{4}}} + \frac{1}{r_{2\bar{3}}} \right) + \alpha_s \frac{1}{2N} \left(\frac{1}{r_{1\bar{3}}} + \frac{1}{r_{2\bar{4}}} - \frac{2}{r_{12}} - \frac{2}{r_{\bar{3}\bar{4}}} \right).
 \end{aligned} \tag{A.9}$$

+/- basis. The last convenient basis for studying the system corresponds to a $\pi/4$ rotation of the Symmetric/Anti-Symmetric basis,

$$\Psi_+ = \frac{1}{\sqrt{2}}(\Psi_S + \Psi_A), \quad \Psi_- = \frac{1}{\sqrt{2}}(\Psi_S - \Psi_A). \tag{A.10}$$

Differently from the previous ones, neither state corresponds to a definite color configuration for a pair of particles. However, they both approach the singlet in the large N limit. In this case, the off-diagonal terms of the Hamiltonian are $1/N$ suppressed with respect to the leading diagonal contributions

$$\begin{aligned}
 V_{++} &= -\alpha_s \frac{N^2-2+N\sqrt{N^2-1}}{4N} \left(\frac{1}{r_{1\bar{3}}} + \frac{1}{r_{2\bar{4}}} \right) - \alpha_s \frac{N^2-2-N\sqrt{N^2-1}}{4N} \left(\frac{1}{r_{2\bar{3}}} + \frac{1}{r_{1\bar{4}}} \right) \\
 &\quad - \alpha_s \frac{1}{2N} \left(\frac{1}{r_{12}} + \frac{1}{r_{\bar{3}\bar{4}}} \right), \\
 V_{+-} &= V_{-+} = \alpha_s \frac{1}{2} \left(\frac{1}{r_{12}} + \frac{1}{r_{\bar{3}\bar{4}}} - \frac{1}{2} \left(\frac{1}{r_{1\bar{3}}} + \frac{1}{r_{1\bar{4}}} + \frac{1}{r_{2\bar{3}}} + \frac{1}{r_{2\bar{4}}} \right) \right), \\
 V_{--} &= -\alpha_s \frac{N^2-2-N\sqrt{N^2-1}}{4N} \left(\frac{1}{r_{1\bar{3}}} + \frac{1}{r_{2\bar{4}}} \right) - \alpha_s \frac{N^2-2+N\sqrt{N^2-1}}{4N} \left(\frac{1}{r_{2\bar{3}}} + \frac{1}{r_{1\bar{4}}} \right) \\
 &\quad - \alpha_s \frac{1}{2N} \left(\frac{1}{r_{12}} + \frac{1}{r_{\bar{3}\bar{4}}} \right).
 \end{aligned} \tag{A.11}$$

B The Born-Oppenheimer approximation

In this appendix, we briefly review the Born-Oppenheimer approximation. A general exposition is beyond the scope of this paper and can be found in textbooks (see, for example [52]).

We will discuss the main aspects of the method by describing an abelian toy example that shares some of the features of the tetraquark system, namely, a hierarchy of masses and a large charge. While some of the results found in this appendix carry over to the non-abelian case, this is not true for others.

B.1 A large N analog of Hydrogen molecule ion

Consider the system of three electrically charged particles. Two of them have mass M and unit charge while the last one has mass m and charge $-N$. We work under the assumptions: $M \gg m$ and $N \gg 1$. The particles interact via Coulombic interactions. The Hamiltonian is then

$$H = \frac{P_1^2}{2M} + \frac{P_2^2}{2M} + \frac{p_3^2}{2m} + \frac{\alpha}{|\vec{R}_1 - \vec{R}_2|} - \frac{\alpha N}{|\vec{r}_3 - \vec{R}_1|} - \frac{\alpha N}{|\vec{r}_3 - \vec{R}_2|}, \quad (\text{B.1})$$

where capital letters are used to denote the heavy particle variables. A convenient change of coordinates allows us to decouple the center of mass motion. The Hamiltonian becomes

$$H = \frac{P_{CM}^2}{2(2M + m)} + \frac{P^2}{M} + \frac{p^2}{2\mu} + \frac{\alpha}{R} - \frac{\alpha N}{|\vec{r} + \frac{1}{2}\vec{R}|} - \frac{\alpha N}{|\vec{r} - \frac{1}{2}\vec{R}|}, \quad (\text{B.2})$$

with the reduced mass $\mu = 2Mm/(2M + m)$. The separation of scales $M \gg m$ suggests the possibility of integrating out the fast modes \vec{p}, \vec{r} and deriving an effective potential for the slow degrees of freedom described by the variables \vec{P}, \vec{R} . Let us follow [46] and write the wavefunction of the full system as a superposition of states

$$\Phi(\vec{r}, \vec{R}) = \sum_{\alpha} \varphi_{\alpha}(\vec{R}) \psi_{\alpha}(\vec{r}; \vec{R}). \quad (\text{B.3})$$

The functions $\{\psi_{\alpha}\}$ are the eigenstates of the light particle Hamiltonian that is

$$\left[\frac{p^2}{2\mu} - \frac{\alpha N}{|\vec{r} + \frac{1}{2}\vec{R}|} - \frac{\alpha N}{|\vec{r} - \frac{1}{2}\vec{R}|} \right] \psi_{\alpha}(\vec{r}; \vec{R}) = E_{\alpha}(\vec{R}) \psi_{\alpha}(\vec{r}; \vec{R}). \quad (\text{B.4})$$

They constitute a complete basis for the fast degrees of freedom. The Schrödinger equation of the full system is then

$$\sum_{\alpha} \left(\frac{P^2}{M} + \frac{\alpha}{R} + E_{\alpha}(R) \right) \varphi_{\alpha}(\vec{R}) \psi_{\alpha}(\vec{r}; \vec{R}) = E \sum_{\alpha} \varphi_{\alpha}(\vec{R}) \psi_{\alpha}(\vec{r}; \vec{R}). \quad (\text{B.5})$$

Note that the electronic eigenstates are normalized according to

$$\int d^3r \psi_{\beta}^e(\vec{r}; \vec{R})^* \psi_{\alpha}(\vec{r}; \vec{R}) = \delta_{\alpha\beta}. \quad (\text{B.6})$$

We multiply eq. (B.4) with $\psi_{\beta}(\vec{r}; \vec{R})^*$ and integrate over r to find

$$\begin{aligned} \int d^3r \psi_{\beta}(\vec{r}; \vec{R})^* \left[2\vec{P}\varphi_{\alpha}(\vec{R}) \cdot \frac{\vec{P}}{M} \psi_{\alpha}(\vec{r}; \vec{R}) + \varphi_{\alpha}(\vec{R}) \frac{P^2}{M} \psi_{\alpha}(\vec{r}; \vec{R}) \right] \\ + \left[\frac{P^2}{M} + V_N(R) + E_{\beta}(R) \right] \varphi_{\beta}(R) = E \varphi_{\beta}(R). \end{aligned} \quad (\text{B.7})$$

The Born-Oppenheimer approximation consists in neglecting the terms in the first line with respect to the first term in the second line, i.e. assuming

$$\int d^3r \psi_\beta(\vec{r}; \vec{R})^* \left[2\vec{P}\varphi_\alpha(\vec{R}) \frac{\vec{P}}{M} \psi_\alpha(\vec{r}; \vec{R}) + \varphi_\alpha(\vec{R}) \frac{P^2}{M} \psi_\alpha(\vec{r}; \vec{R}) \right] \ll \frac{P^2}{M} \varphi_\alpha(\vec{R}). \quad (\text{B.8})$$

As we have $P\varphi_\alpha(\vec{R}) \sim P_N\varphi_\alpha(\vec{R})$, where P_N is the typical nucleon momentum, and we generically expect $P\psi(\vec{r}; \vec{R}) \sim p_e\psi(\vec{r}; \vec{R})$ as well as $P^2\psi(\vec{r}; \vec{R}) \sim p_e^2\psi(\vec{r}; \vec{R})$ with p_e the typical electron momentum,¹² this is a good approximation as long as

$$p_e \ll P_N, \quad (\text{B.9})$$

a condition that we can check a posteriori.

Thus, in the Born-Oppenheimer approximation, we are left with the reduced nuclear problem with Hamiltonian

$$H = \frac{P^2}{M} + \frac{\alpha}{R} + V(R), \quad (\text{B.10})$$

with the effective potential computed as the eigenvalue of the electronic ground state with the nuclei treated as static sources. The large N limit allows to solve for $\psi_\alpha(\vec{r}; \vec{R})$, and thus also $V(R)$ perturbatively.¹³ This comes from the fact that due to the large charge of the light particle, the two heavy particles will self-consistently be localized at distances R_0 much shorter than the typical Bohr radius of the light particle a_0 . Assuming that this is indeed the case, one can easily solve for the wavefunction of the light particle perturbatively and in the end check for self-consistency. To leading order we treat the two heavy particles as being at the same position. The solution for the light particle is then just a Hydrogen wavefunction around a nucleus with charge 2, i.e. with Bohr radius $a_0 = 1/(2N\alpha m)$, and ground state energy

$$E_0 = 2Nm\alpha^2 \quad (\text{B.11})$$

This energy is independent of R , while the leading R dependence is $\mathcal{O}(R^2)$ and can be found using the first order perturbation theory in terms of the following perturbation Hamiltonian

$$\Delta V \equiv \frac{2Q\alpha}{r} - \frac{Q\alpha}{|\vec{r} - \vec{R}/2|} - \frac{Q\alpha}{|\vec{r} + \vec{R}/2|}, \quad (\text{B.12})$$

and one finds

$$\Delta E(R) = \frac{1}{3}E_0 \frac{R^2}{a_0^2} + \mathcal{O}\left(E_0 \frac{R^3}{a_0^3}\right) \quad (\text{B.13})$$

This acts as a BO potential for the heavy particles, and the reduced problem is

$$\left[-\frac{\nabla_{\vec{R}}^2}{M} + \frac{\alpha}{R} + \Delta E(R) \right] \varphi(\vec{R}) = E\varphi(\vec{R}). \quad (\text{B.14})$$

¹²There are however situations in which $P\psi(\vec{r}; \vec{R}) \ll p_e\psi(\vec{r}; \vec{R})$, however typically one still has $P^2\psi(\vec{r}; \vec{R}) \sim p_e^2\psi(\vec{r}; \vec{R})$. One such situation is exactly the example described in this appendix.

¹³Note that this is the difference with respect to the often discussed H_2^+ , in which no similar expansion parameter exists. There the electronic system is either solved numerically with the help of cylindrical symmetry, or by making the ansatz of orbitals. In contrast, in the large N limit, we can find the analytic solution in perturbation theory.

The minimum of the potential is at $R_0 = a_0 \left(\frac{3}{2N}\right)^{1/3}$, thus for verifying our assumptions of $R_0 \ll a_0$ for $N \gg 1$. On top of that, the condition for the validity of the BO approximation can be checked explicitly and is found to be $m/M \ll 1$. This is in contrast to the scaling in the main text, where the BO approximation is only valid for $Nm/M \ll 1$. The difference stems from the fact that in the non-abelian case the perturbatively generated potential is down by an additional factor of N , while here it is of leading order in the N counting.

C Analytic form of the Born-Oppenheimer potential

In section 3 we found an analytic expression for the BO potentials in the limit $\frac{m_4}{m_3} \rightarrow 0$. In this appendix, we provide the corrections to this expressions for small but nonzero $\frac{m_4}{m_3}$. Recall that the BO potentials can be written in terms of $\Delta(R)$ defined in eq. (3.15) as $V_{\text{BO}} = \pm \frac{1}{N} \Delta(R)$. The integral expression for $\Delta(R)$ is given by

$$\begin{aligned} \frac{\Delta(R)}{\mathcal{E}_3} &= \frac{2}{\pi^2 a_3^5} \left(\frac{m_4}{m_3}\right)^3 \int d^3 r_3 d^3 r_4 e^{-(r_{13}+r_{23})/a_3} e^{-\frac{m_4}{m_3}(r_{14}+r_{24})/a_3} \\ &\quad \times \left[\frac{1}{r_{12}} + \frac{1}{r_{34}} - \frac{1}{2} \left(\frac{1}{r_{13}} + \frac{1}{r_{24}} + \frac{1}{r_{14}} + \frac{1}{r_{23}} \right) \right]. \end{aligned} \quad (\text{C.1})$$

All the terms have a simple analytic form except the following:

$$I_{34}(R) = \frac{2}{\pi^2 a_3^5} \left(\frac{m_4}{m_3}\right)^3 \int d^3 r_3 d^3 r_4 \frac{1}{r_{34}} e^{-(r_{13}+r_{23})/a_3} e^{-\frac{m_4}{m_3}(r_{14}+r_{24})/a_3}. \quad (\text{C.2})$$

The BO potential can thus be written as

$$\begin{aligned} \frac{\Delta(R)}{\mathcal{E}_3} &= I_{34}(R) + 2e^{-\left(1+\frac{m_4}{m_3}\right)\frac{R}{a_3}} \left[\frac{a_3}{R} - \frac{1}{3} \left(2 + 3\frac{m_4}{m_3} + 3\left(\frac{m_4}{m_3}\right)^2 \right) \frac{R}{a_3} \right. \\ &\quad \left. - \frac{m_4}{m_3} \left(\frac{m_4}{m_3} + 1 \right) \left(\frac{R}{a_3} \right)^2 - \frac{5}{9} \left(\frac{m_4}{m_3} \right)^2 \left(\frac{R}{a_3} \right)^3 \right]. \end{aligned} \quad (\text{C.3})$$

$I_{34}(R)$ can be computed for $m_4/m_3 \ll 1$ in a perturbative expansion in m_4/m_3 . The leading-order term is proportional to m_4/m_3 . This term cancels out exactly with the term of the same order found in eq. (C.3). The next correction to $I_{34}(R)$ is of order $(m_4/m_3)^3$. Thus, in the $m_4/m_3 \ll 1$, the BO potential is found to be

$$\frac{\Delta(R)}{\mathcal{E}_3} = 2e^{-\frac{R}{a_3}} \left(\frac{a_3}{R} - \frac{2R}{3a_3} - \frac{1}{2} \left(\frac{m_4}{m_3} \right)^2 \frac{R}{a_3} + \frac{1}{9} \left(\frac{m_4}{m_3} \right)^2 \left(\frac{R}{a_3} \right)^3 \right) + \mathcal{O} \left(\left(\frac{m_4}{m_3} \right)^3 \right). \quad (\text{C.4})$$

D Effects of the excited states

In this appendix we discuss the effects of the excited states by estimating their contribution to the effective Hamiltonian governing the dynamics of the low energy part of the spectrum. In section 4, we showed that considering only states constructed as superpositions of the ground state mesons, ground state tetraquarks cannot form for the hierarchy $M_2 \ll Nm_3$. We will argue in this appendix that including the contribution of the excited states to the low energy

dynamics also does not lead to formation of tetraquark ground states. For this argument, in addition to the mass hierarchy $M_2 \ll Nm$, we assume that the modification of the spectrum of the excited states due to the potential at subleading $1/N$ orders does not remove their energy gap (from the ground state level of the leading Hamiltonian).

Using the eigenstates of the Hamiltonian H'_0 , we can write the Hilbert space as the direct sum of a ground state sector and a sector of excited state Hilbert space, $\mathcal{H} = \mathcal{H}_{\text{GS}} \oplus \mathcal{H}_{\text{exc}}$, and denote the respective projection operators as \mathbb{P}_{GS} and \mathbb{P}_{exc} , such that

$$\mathbb{P}_{\text{GS}} + \mathbb{P}_{\text{ES}} = \mathbb{I} \tag{D.1}$$

The Hamiltonian can be represented as

$$H' = \begin{pmatrix} H_{\text{GS}} & H_{\text{mix}} \\ H_{\text{mix}}^\dagger & H_{\text{exc}} \end{pmatrix}, \tag{D.2}$$

where $H_{\text{GS}} = \mathbb{P}_{\text{GS}} H' \mathbb{P}_{\text{GS}}$ and $H_{\text{exc}} = \mathbb{P}_{\text{exc}} H' \mathbb{P}_{\text{exc}}$ are the projected Hamiltonian into the two subspaces and the mixing is governed only by the terms of the potential subleading in $1/N$,

$$H_{\text{mix}} = \frac{1}{N} \mathbb{P}_{\text{GS}} V^{(1)} \mathbb{P}_{\text{exc}} + \mathcal{O}(1/N^2). \tag{D.3}$$

According to the standard Green's function approach (see for instance [53]) time evolution in the \mathcal{H}_{GS} low energy subspace is governed by the effective Hamiltonian is then given by

$$H_{\text{eff}}(E) = H_{\text{GS}} + \frac{1}{N^2} \mathbb{P}_{\text{GS}} V^{(1)} \mathbb{P}_{\text{exc}} \frac{1}{E - H_{\text{exc}} + i\varepsilon} \mathbb{P}_{\text{exc}} V^{(1)} \mathbb{P}_{\text{GS}} \tag{D.4}$$

The first term includes the leading Hamiltonian as well as the potential projected in the subspace of ground state, the effects of which were shown to not lead to bound states for $M_2 \ll Nm_{\bar{3}}$ in section 4. We now focus on the second term which gives the contribution of the states above the gap to the effective Hamiltonian. For simplicity of the presentation, we take $m_{\bar{4}} \sim m_{\bar{3}}$ and therefore $\mathcal{E}_{\bar{3}} \sim \mathcal{E}_{\bar{4}}$. The spectrum of the leading order part of H_{exc} , is bounded from below by $E_{\text{exc}} \gtrsim \mathcal{E}_{\bar{3}}$. We assume that this gap persists also after the $1/N$ corrections are included. With this assumption, the second term above is negative definite and its magnitude can be bounded by

$$V^{(1)} \mathbb{P}_{\text{ES}} \frac{1}{-E + H_{\text{ES}}} \mathbb{P}_{\text{ES}} V^{(1)} \lesssim \frac{V^{(1)} \mathbb{P}_{\text{ES}} V^{(1)}}{\mathcal{E}_{\bar{3}}} \tag{D.5}$$

We can estimate the matrix elements of the right hand side of the equation above in the basis $|s, \vec{R}_s, GS\rangle$ with $s = A, B$. This has vanishing matrix elements between two different sectors A and B since it has two factors of the potential and the potential $V^{(1)}$ is purely sector-off-diagonal. Using eq. (D.1), it can be split into two terms

$$V^{(1)} \mathbb{P}_{\text{ES}} V^{(1)} = V^{(1)} V^{(1)} - V^{(1)} \mathbb{P}_{\text{GS}} V^{(1)} \tag{D.6}$$

which we now study separately. We only quote the expressions for the matrix elements in the A sector for which given the basis we have chosen, with each meson of the A sector in a color-singlet state, the fall-off of the interaction at large distance is manifest. Similar

results hold for the B sector, although the quick fall off of the interaction at large distance is not manifest in the basis eq. (A.9)

The matrix elements of the first of eq. (D.6) term are

$$\langle A, \vec{R}'_A, GS | (V^{(1)})^2 | A, \vec{R}_A, GS \rangle \simeq \mathcal{E}_3^2 F(R_A/a_3) \delta^3(\vec{R}_A - \vec{R}'_A) \quad (\text{D.7})$$

The approximation works in the regime defined by equation eq. (4.14), see also footnote 10. The $F(R_A/a_3)$ can be estimated to be

$$F(R_A/a_3) \sim \begin{cases} (a_3/R_A)^2 & R_A \lesssim a_3, \\ (a_3/R_A)^6 & R_A \gtrsim a_3. \end{cases} \quad (\text{D.8})$$

The small $R_A \ll a_3$ is dominated by the contribution of the term proportional to $1/r_{12}$ in the potential, while the large $R_A \gg a_3$ can be understood from eq. (4.4) where for $r_{13}, r_{24} \ll r_{12}$ the potential has a dipole-dipole interaction $\propto 1/r_{12}^3$. We now find the matrix elements of the second term of eq. (D.6) by inserting a complete basis of states in the ground state mesons sector

$$\begin{aligned} & \langle A, \vec{R}'_A, GS | V^{(1)} \mathbb{P}_{\text{GS}} V^{(1)} | A, \vec{R}_A, GS \rangle \\ &= \int d^3 R_B \langle A, \vec{R}'_A, GS | V^{(1)} | B, \vec{R}_B, GS \rangle \langle B, \vec{R}_B, GS | V^{(1)} | A, \vec{R}_A, GS \rangle \\ &= \delta^3(\vec{R}_A - \vec{R}'_A) \Delta(R_A)^2 \end{aligned} \quad (\text{D.9})$$

where we used eq. (4.16). Note that $\Delta(R_A)^2$ is $1/R_A^2$ for $R_A \ll a_3$ which is dominated by the contribution of the term proportional to $1/r_{12}$ in the potential. This indeed cancels the leading short distance $\propto 1/R_A^2$ contribution of $F(R_A/a_3)$. To see this more clearly, note that the ground state mesons in the basis labelled by \vec{R}_A are approximate eigenstates of the $\propto 1/r_{12}$ term in the potential and hence this term leaves a state in the ground state sector in \mathcal{H}_{GS} so that the action of the projector \mathbb{P}_{ES} gives a vanishing result. For the same reason, there are no terms $\propto 1/R_A$ in the full matrix element. Therefore, the effect of the second term in eq. (D.4) is bounded by a potential which in the A sector is estimated as

$$\begin{cases} \frac{\mathcal{E}_3}{N^2} & R_A \lesssim a_3, \\ \frac{\mathcal{E}_3}{N^2} (a_3/R_A)^6 & R_A \gtrsim a_3. \end{cases} \quad (\text{D.10})$$

From the Bargmann-Schwinger condition, eq. (3.21), it is then obvious that these contribution cannot lead to formation of the bound states as long as $M_2/m_3 \ll N^2$. As already stated above, we only showed the matrix elements in the A sector. For the B sector, the short distance behavior is reproduced identically following the same steps. But the long distance $\propto 1/R^6$ fall off is not manifest since in the basis we have chosen the mesons of the B sector are color-singlets only at leading order in $1/N$. However had we chosen a basis defined by $(Q_1 \bar{q}_4)$ and $(Q_2 \bar{q}_3)$ pairs being both in the singlet or both in the adjoint color representations, the fall of would be manifest in the effective description for the B sector mesons.

Data Availability Statement. This article has no associated data or the data will not be deposited.

Code Availability Statement. This article has no associated code or the code will not be deposited.

Open Access. This article is distributed under the terms of the Creative Commons Attribution License ([CC-BY4.0](https://creativecommons.org/licenses/by/4.0/)), which permits any use, distribution and reproduction in any medium, provided the original author(s) and source are credited.

References

- [1] BELLE collaboration, *Observation of a narrow charmonium-like state in exclusive $B^\pm \rightarrow K^\pm \pi^+ \pi^- J/\psi$ decays*, *Phys. Rev. Lett.* **91** (2003) 262001 [[hep-ex/0309032](https://arxiv.org/abs/hep-ex/0309032)] [[INSPIRE](https://inspirehep.net/literature/1000000)].
- [2] A. Esposito, A. Pilloni and A.D. Polosa, *Multiquark Resonances*, *Phys. Rept.* **668** (2017) 1 [[arXiv:1611.07920](https://arxiv.org/abs/1611.07920)] [[INSPIRE](https://inspirehep.net/literature/1611079)].
- [3] F.-K. Guo et al., *Hadronic molecules*, *Rev. Mod. Phys.* **90** (2018) 015004 [Erratum *ibid.* **94** (2022) 029901] [[arXiv:1705.00141](https://arxiv.org/abs/1705.00141)] [[INSPIRE](https://inspirehep.net/literature/1705004)].
- [4] S.L. Olsen, T. Skwarnicki and D. Zieminska, *Nonstandard heavy mesons and baryons: Experimental evidence*, *Rev. Mod. Phys.* **90** (2018) 015003 [[arXiv:1708.04012](https://arxiv.org/abs/1708.04012)] [[INSPIRE](https://inspirehep.net/literature/1708040)].
- [5] N. Brambilla et al., *The XYZ states: experimental and theoretical status and perspectives*, *Phys. Rept.* **873** (2020) 1 [[arXiv:1907.07583](https://arxiv.org/abs/1907.07583)] [[INSPIRE](https://inspirehep.net/literature/1907075)].
- [6] LHCb collaboration, *Observation of an exotic narrow doubly charmed tetraquark*, *Nature Phys.* **18** (2022) 751 [[arXiv:2109.01038](https://arxiv.org/abs/2109.01038)] [[INSPIRE](https://inspirehep.net/literature/2109038)].
- [7] LHCb collaboration, *Study of the doubly charmed tetraquark T_{cc}^+* , *Nature Commun.* **13** (2022) 3351 [[arXiv:2109.01056](https://arxiv.org/abs/2109.01056)] [[INSPIRE](https://inspirehep.net/literature/2109056)].
- [8] LHCb collaboration, *Observation of structure in the J/ψ -pair mass spectrum*, *Sci. Bull.* **65** (2020) 1983 [[arXiv:2006.16957](https://arxiv.org/abs/2006.16957)] [[INSPIRE](https://inspirehep.net/literature/2006169)].
- [9] A.V. Manohar and M.B. Wise, *Heavy Quark Physics*, *Camb. Monogr. Part. Phys. Nucl. Phys. Cosmol.*, Cambridge University Press (2000).
- [10] D.B. Kaplan, *Five lectures on effective field theory*, [nucl-th/0510023](https://arxiv.org/abs/hep-th/0510023) [[INSPIRE](https://inspirehep.net/literature/1000000)].
- [11] E.J. Eichten and C. Quigg, *Heavy-quark symmetry implies stable heavy tetraquark mesons $Q_i Q_j \bar{q}_k \bar{q}_l$* , *Phys. Rev. Lett.* **119** (2017) 202002 [[arXiv:1707.09575](https://arxiv.org/abs/1707.09575)] [[INSPIRE](https://inspirehep.net/literature/1707095)].
- [12] E. Braaten, L.-P. He and A. Mohapatra, *Masses of doubly heavy tetraquarks with error bars*, *Phys. Rev. D* **103** (2021) 016001 [[arXiv:2006.08650](https://arxiv.org/abs/2006.08650)] [[INSPIRE](https://inspirehep.net/literature/2006086)].
- [13] S. Fleming, M. Kusunoki, T. Mehen and U. van Kolck, *Pion interactions in the $X(3872)$* , *Phys. Rev. D* **76** (2007) 034006 [[hep-ph/0703168](https://arxiv.org/abs/hep-ph/0703168)] [[INSPIRE](https://inspirehep.net/literature/1460000)].
- [14] E. Braaten and M. Kusunoki, *Low-energy universality and the new charmonium resonance at 3870-MeV*, *Phys. Rev. D* **69** (2004) 074005 [[hep-ph/0311147](https://arxiv.org/abs/hep-ph/0311147)] [[INSPIRE](https://inspirehep.net/literature/1000000)].
- [15] E. Braaten, *Galilean-invariant effective field theory for the $X(3872)$* , *Phys. Rev. D* **91** (2015) 114007 [[arXiv:1503.04791](https://arxiv.org/abs/1503.04791)] [[INSPIRE](https://inspirehep.net/literature/1300000)].
- [16] G. 't Hooft, *A Planar Diagram Theory for Strong Interactions*, *Nucl. Phys. B* **72** (1974) 461 [[INSPIRE](https://inspirehep.net/literature/1000000)].
- [17] E. Witten, *Baryons in the $1/n$ Expansion*, *Nucl. Phys. B* **160** (1979) 57 [[INSPIRE](https://inspirehep.net/literature/1000000)].
- [18] S. Coleman, *Aspects of Symmetry: Selected Erice Lectures*, Cambridge University Press, Cambridge, U.K. (1985) [[DOI:10.1017/CB09780511565045](https://doi.org/10.1017/CB09780511565045)] [[INSPIRE](https://inspirehep.net/literature/1000000)].

- [19] S. Weinberg, *Tetraquark Mesons in Large N Quantum Chromodynamics*, *Phys. Rev. Lett.* **110** (2013) 261601 [[arXiv:1303.0342](#)] [[INSPIRE](#)].
- [20] M. Knecht and S. Peris, *Narrow Tetraquarks at Large N* , *Phys. Rev. D* **88** (2013) 036016 [[arXiv:1307.1273](#)] [[INSPIRE](#)].
- [21] L. Maiani, A.D. Polosa and V. Riquer, *Tetraquarks in the $1/N$ Expansion: a New Appraisal*, *Phys. Rev. D* **98** (2018) 054023 [[arXiv:1803.06883](#)] [[INSPIRE](#)].
- [22] T.D. Cohen and R.F. Lebed, *Are There Tetraquarks at Large N_c in QCD(F)?*, *Phys. Rev. D* **90** (2014) 016001 [[arXiv:1403.8090](#)] [[INSPIRE](#)].
- [23] A. Ali, L. Maiani and A.D. Polosa, *Multiquark Hadrons*, Cambridge University Press (2019).
- [24] W. Lucha, D. Melikhov and H. Sazdjian, *Tetraquarks in large- N_c QCD*, *Prog. Part. Nucl. Phys.* **120** (2021) 103867 [[arXiv:2102.02542](#)] [[INSPIRE](#)].
- [25] A. Armoni, M. Shifman and G. Veneziano, *SUSY relics in one flavor QCD from a new $1/N$ expansion*, *Phys. Rev. Lett.* **91** (2003) 191601 [[hep-th/0307097](#)] [[INSPIRE](#)].
- [26] T.D. Cohen and R.F. Lebed, *Tetraquarks with exotic flavor quantum numbers at large N_c in QCD(AS)*, *Phys. Rev. D* **89** (2014) 054018 [[arXiv:1401.1815](#)] [[INSPIRE](#)].
- [27] T. Cohen, F.J. Llanes-Estrada, J.R. Pelaez and J. Ruiz de Elvira, *Nonordinary light meson couplings and the $1/N_c$ expansion*, *Phys. Rev. D* **90** (2014) 036003 [[arXiv:1405.4831](#)] [[INSPIRE](#)].
- [28] J.P. Ader, J.M. Richard and P. Taxil, *Do narrow heavy multi-quark states exist?*, *Phys. Rev. D* **25** (1982) 2370 [[INSPIRE](#)].
- [29] H.J. Lipkin, *A model independent approach to multi-quark bound states*, *Phys. Lett. B* **172** (1986) 242 [[INSPIRE](#)].
- [30] J. Carlson, L. Heller and J.A. Tjon, *Stability of Dimesons*, *Phys. Rev. D* **37** (1988) 744 [[INSPIRE](#)].
- [31] A.V. Manohar and M.B. Wise, *Exotic $QQqq$ states in QCD*, *Nucl. Phys. B* **399** (1993) 17 [[hep-ph/9212236](#)] [[INSPIRE](#)].
- [32] SELEX collaboration, *First Observation of the Doubly Charmed Baryon Ξ_{cc}^+* , *Phys. Rev. Lett.* **89** (2002) 112001 [[hep-ex/0208014](#)] [[INSPIRE](#)].
- [33] SELEX collaboration, *Confirmation of the double charm baryon $\Xi_{cc}^+(3520)$ via its decay to pD^+K^-* , *Phys. Lett. B* **628** (2005) 18 [[hep-ex/0406033](#)] [[INSPIRE](#)].
- [34] B.A. Gelman and S. Nussinov, *Does a narrow tetraquark cc anti- u anti- d state exist?*, *Phys. Lett. B* **551** (2003) 296 [[hep-ph/0209095](#)] [[INSPIRE](#)].
- [35] LHCb collaboration, *Observation of the doubly charmed baryon Ξ_{cc}^{++}* , *Phys. Rev. Lett.* **119** (2017) 112001 [[arXiv:1707.01621](#)] [[INSPIRE](#)].
- [36] M. Karliner and J.L. Rosner, *Discovery of doubly-charmed Ξ_{cc} baryon implies a stable $(bb\bar{u}\bar{d})$ tetraquark*, *Phys. Rev. Lett.* **119** (2017) 202001 [[arXiv:1707.07666](#)] [[INSPIRE](#)].
- [37] H. An and M.B. Wise, *The Direct Coupling of Light Quarks to Heavy Di-quarks*, *Phys. Lett. B* **788** (2019) 131 [[arXiv:1809.02139](#)] [[INSPIRE](#)].
- [38] A. Czarnecki, B. Leng and M.B. Voloshin, *Stability of tetrons*, *Phys. Lett. B* **778** (2018) 233 [[arXiv:1708.04594](#)] [[INSPIRE](#)].
- [39] E. Braaten, C. Langmack and D.H. Smith, *Born-Oppenheimer Approximation for the XYZ Mesons*, *Phys. Rev. D* **90** (2014) 014044 [[arXiv:1402.0438](#)] [[INSPIRE](#)].

- [40] S. Prelovsek, H. Bahtiyar and J. Petkovic, *Zb tetraquark channel from lattice QCD and Born-Oppenheimer approximation*, *Phys. Lett. B* **805** (2020) 135467 [[arXiv:1912.02656](#)] [[INSPIRE](#)].
- [41] M. Sadl and S. Prelovsek, *Tetraquark channels with $\bar{b}b$ pair in the static limit*, *PoS LATTICE2021* (2022) 427 [[arXiv:2110.14568](#)] [[INSPIRE](#)].
- [42] EUROPEAN TWISTED MASS collaboration, *Lattice QCD signal for a bottom-bottom tetraquark*, *Phys. Rev. D* **87** (2013) 114511 [[arXiv:1209.6274](#)] [[INSPIRE](#)].
- [43] P. Bicudo, *Tetraquarks and pentaquarks in lattice QCD with light and heavy quarks*, *Phys. Rept.* **1039** (2023) 1 [[arXiv:2212.07793](#)] [[INSPIRE](#)].
- [44] F. Alasiri, E. Braaten and A. Mohapatra, *Born-Oppenheimer potentials for SU(3) gauge theory*, *Phys. Rev. D* **110** (2024) 054029 [[arXiv:2406.05123](#)] [[INSPIRE](#)].
- [45] L. Maiani, A.D. Polosa and V. Riquer, *Hydrogen bond of QCD*, *Phys. Rev. D* **100** (2019) 014002 [[arXiv:1903.10253](#)] [[INSPIRE](#)].
- [46] S. Weinberg, *Approximations for energy eigenvalues*, in *Lectures on Quantum Mechanics*, p. 169-213, Cambridge University Press (2015) [[DOI:10.1017/CB09781316276105.007](#)].
- [47] V. Bargmann, *On the Number of Bound States in a Central Field of Force*, *Proc. Nat. Acad. Sci.* **38** (1952) 961.
- [48] J. Schwinger, *On the bound states of a given potential*, *Proc. Nat. Acad. Sci.* **47** (1961) 122.
- [49] S. Meinel, M. Pflaumer and M. Wagner, *Search for $\bar{b}b_{us}$ and $\bar{b}c_{ud}$ tetraquark bound states using lattice QCD*, *Phys. Rev. D* **106** (2022) 034507 [[arXiv:2205.13982](#)] [[INSPIRE](#)].
- [50] A. Francis, R.J. Hudspith, R. Lewis and K. Maltman, *Lattice Prediction for Deeply Bound Doubly Heavy Tetraquarks*, *Phys. Rev. Lett.* **118** (2017) 142001 [[arXiv:1607.05214](#)] [[INSPIRE](#)].
- [51] P. Junnarkar, N. Mathur and M. Padmanath, *Study of doubly heavy tetraquarks in Lattice QCD*, *Phys. Rev. D* **99** (2019) 034507 [[arXiv:1810.12285](#)] [[INSPIRE](#)].
- [52] S. Weinberg, *Lectures on quantum mechanics*, Cambridge University Press (2015).
- [53] M. Mariño, *Advanced Topics in Quantum Mechanics*, Cambridge University Press (2021) [[DOI:10.1017/9781108863384](#)] [[INSPIRE](#)].